

Observational and model evidence for a prominent stratospheric influence on variability in tropospheric nitrous oxide

Cynthia D. Nevison¹, Qing Liang², Paul A. Newman², Britton B. Stephens³, Geoff Dutton^{4,5}, Xin Lan^{4,5}, Roisin Commane⁶, Yenny Gonzalez^{7,8}, Eric Kort⁹

¹Institute for Arctic and Alpine Research, University of Colorado, Boulder, CO, USA

²NASA Goddard Space Flight Center, Greenbelt, MD, USA

³NSF National Center for Atmospheric Research, Boulder, CO, USA

⁴Global Monitoring Laboratory, NOAA Earth System Research Laboratory, Boulder, CO, USA

⁵Cooperative Institute for Research in Environmental Sciences (CIRES), University of Colorado, Boulder, CO, USA

⁶Department of Earth & Environmental Sciences, Lamont-Doherty Earth Observatory, Columbia University, Palisades, NY, USA

⁷CIMEL Electronique, Paris, 75011, France

⁸Izana Atmospheric Research Center, AEMET, Santa Cruz de Tenerife, 38001, Spain

⁹Department of Climate & Space Sciences & Engineering, University of Michigan, Ann Arbor, MI, USA

Correspondence to: Cynthia D. Nevison (cynthia.nevison@colorado.edu)

Abstract

The literature presents differing views on how variability in surface nitrous oxide (N₂O) is influenced by the stratosphere and whether forcings associated with the El Niño Southern Oscillation (ENSO) outweigh those influences. These issues are relevant to interpreting biogeochemical source signals in tropospheric N₂O and are investigated here using surface and aircraft-based atmospheric N₂O measurements and a chemistry-climate model with a stratospheric N₂O tracer. The model simulates well-defined seasonal cycles in tropospheric N₂O that are predominantly caused by the seasonal descent of N₂O-poor stratospheric air in polar regions with subsequent cross-tropopause transport and mixing. Similar cycles are identified in recently available data from global airborne surveys and aircraft-based monitoring. In the northern hemisphere, the annually-averaged surface N₂O atmospheric growth rate anomaly derived from long-term monitoring data is negatively correlated with winter (January-March) polar lower stratospheric temperature. This correlation is consistent with an influence from the Brewer Dobson circulation, which brings warm, N₂O-poor air from the middle and upper stratosphere into the lower stratosphere. In the southern hemisphere, the atmospheric growth rate anomaly is better correlated

Deleted: Northern vs. southern hemisphere differences in the

Deleted: .

Formatted: Line spacing: 1.5 lines

Formatted: Font: Not Bold, Not Italic

Formatted: Font: Not Bold, Not Italic

Formatted: Font: Not Bold, Not Italic

Formatted: Font: Not Bold, Not Italic

Formatted: Font: Not Bold, Not Italic

Formatted: Font: Not Bold, Not Italic

Deleted: We presen

Deleted: t

Formatted: Font: Not Bold, Not Italic

Formatted: Subscript

Deleted: tagged

Deleted: nitrous oxide (

Deleted:)

Deleted: that

Deleted: predicts

Deleted: distinct

Deleted: depleted

Deleted: We identify s

Deleted: phenomena

Deleted: aircraft profiles

Deleted: campaigns

Deleted: routine

Deleted: Long-term atmospheric measurements from the National Oceanic Atmospheric Administration (NOAA) global surface monitoring network provide additional support for a significant impact on surface N₂O originating from the stratosphere.

Deleted: I

Deleted: NOAA

Deleted:

Deleted: the previous winter's

Deleted: .

Deleted: This negative correlation is consistent with increa... [1]

Deleted: of

Deleted: depleted

Deleted: , with subsequent cross-tropopause transport of th... [2]

Deleted: However,

Deleted: N₂O

Deleted: in the southern hemisphere

to indices of ENSO and the stratospheric quasi-biennial oscillation (QBO). These hemispheric differences in the factors influencing the N₂O growth rate are consistent with known atmospheric dynamics and the complex interaction of the QBO with the Brewer Dobson circulation. More airborne surveys, which provide high-resolution N₂O data near the tropopause, would help refine our understanding of the stratospheric influence on the troposphere and enhance our ability to interpret surface N₂O sources.

1 Introduction

Nitrous oxide (N₂O) is an important ozone-depleting substance and long-lived greenhouse gas, with a global warming potential (GWP) of 265 relative to CO₂ over a 100 year time horizon (WMO, 2018). N₂O has an atmospheric lifetime of about 120 years and is destroyed slowly in the stratosphere by both photolysis and oxidation, with a fraction of the oxidation product yielding NO_x, a catalyst of stratospheric ozone destruction (Crutzen, 1970; Prather et al., 2015). N₂O has abundant natural microbial sources in soil, freshwater and oceans, which account for the majority of global emissions, although anthropogenic sources are becoming increasingly important (Tian et al., 2020; Canadell et al., 2021).

The atmospheric N₂O concentration has risen from about ~270 ppb preindustrially to 336 ppb by 2022 (MacFarling-Meure et al., 2006; Lan et al., 2022). This rise has been attributed largely to Haber-Bosch industrial N fixation to produce agricultural fertilizer, which has increased the substrate available to nitrogen (N) cycling microbes (Park et al., 2012). Recent evidence suggests that N₂O is increasing at an accelerating rate in the atmosphere, possibly due to a nonlinear response of microbes to increasing N inputs in intensively fertilized agricultural systems (Thompson et al., 2019; Liang et al., 2022).

High precision measurements of N₂O have revealed interannual variability in its atmospheric growth rate (AGR) and small-amplitude seasonal cycles in the range of 0.4 to 1 ppb (Nevison et al., 2004; 2007; 2011; Jiang et al., 2007; Thompson et al., 2013). Spatial gradients in atmospheric N₂O are also small, e.g., the northern hemisphere (NH) minus southern hemisphere (SH) difference is approximately 1 ppb

Deleted: the

Deleted: index, as well as the El Niño Southern Oscillation index, than to polar lower stratospheric temperature

Deleted:

Deleted: atmospheric

Formatted: Font: (Default) +Headings (Times New Roman), 12 pt

Formatted: Font: 12 pt

Formatted: Font: 12 pt

Formatted: Font: 12 pt

Formatted: Font: (Default) +Headings (Times New Roman), 12 pt

Formatted: Font: 12 pt

Formatted: Font: (Default) +Headings (Times New Roman), 12 pt

Formatted: Font: (Default) +Headings (Times New Roman), 12 pt

Formatted: Subscript

Formatted: Font: (Default) +Headings (Times New Roman), 12 pt

Formatted: Font: (Default) +Headings (Times New Roman)

Formatted: Font: 12 pt

Formatted: Line spacing: 1.5 lines

Formatted: Font: Italic

Deleted: the

Deleted: process of

Deleted: for the

Deleted: tion of

Deleted: N

Deleted: I

Deleted: the

Formatted: Subscript

Deleted: (

Deleted: 0.1 – 0.3% of the background mixing ratio) are detectable in the high precision N₂O measurements made in recent decades ...

Deleted:

Formatted: Font: Not Bold

Formatted: Font: Not Bold

Formatted: Font: Not Bold, Subscript

Formatted: Font: Not Bold

Formatted: Font: Not Bold

(Thompson et al., 2014b; Liang et al., 2022). While larger spatial and seasonal signals in atmospheric N₂O have been observed at sites influenced by strong local agricultural or coastal upwelling sources (Lueker et al., 2003; Nevison et al., 2018; Ganesan et al., 2020), at sites remote from local sources even variations of 0.2 ppb in estimated background N₂O levels can significantly affect the magnitude of N₂O emissions inferred from atmospheric inversions (Nevison et al., 2018).

Formatted: Font: Not Bold

Formatted: Font: Not Bold

Formatted: Font: Not Bold, Subscript

Formatted: Font: Not Bold

A few studies have inferred information about surface biogeochemical sources based on the observed seasonal cycle in atmospheric N₂O at remote monitoring sites. However, these studies have cautioned that the transport of N₂O-poor air from the stratosphere is a major cause of both seasonal and interannual variability in surface N₂O, which complicates the interpretation of surface emission signals (Nevison et al., 2005; 2011; 2012; Thompson et al., 2014b; Ray et al., 2020; Ruiz et al., 2021). Other studies have argued that El Niño Southern Oscillation (ENSO) cycles are the major driver of interannual variability in tropospheric N₂O (Ishijima et al., 2009; Thompson et al., 2013; Canadell et al., 2021) or that ENSO-driven variability can obscure the influence of the stratosphere in some years (Ruiz et al., 2021). ENSO refers to the periodic oscillation between warm (El Niño) and cold (La Niña) phases in the eastern tropical Pacific (ETP). During the El Niño phase, the warming and deepening of the thermocline is associated with reduced upwelling in the ETP and drought in South America, which can decrease oceanic and soil N₂O emissions, respectively (McPhadden et al., 1998; Ishijima et al., 2009; Babbitt et al., 2015).

Deleted: depleted

Deleted: likely

Deleted:

Formatted: Subscript

Formatted: Font: Italic

Deleted: N

Deleted: H

Deleted: vs.

Deleted: S

Deleted: H

Deleted: QBO at 50 hPa

Deleted: NOAA

Deleted: station

Deleted: but

Deleted: They hypothesized that the correlation of QBO and N₂O AGR was less evident in the NH due to the increased influence of surface emissions.

Deleted: QBO

Deleted: to

Deleted: at the surface

Deleted: stratosphere

Deleted: sphere

Studies of the stratospheric influence on surface N₂O variability have differed with respect to the relative impact on the northern hemisphere (NH) and southern hemisphere (SH). Ray et al. (2020) found direct correlations between the stratospheric Quasi-Biennial Oscillation (QBO), lagged 8-12 months, and the observed surface N₂O AGR, but in the SH only. The QBO is a tropical, stratospheric, downward-propagating zonal wind variation with an average period of ~28 months that dominates the variability of tropical lower stratospheric meteorology (Baldwin et al., 2001; Butchart, 2014). Ruiz et al. (2021) found that, despite a clear correlation between the QBO and N₂O photochemical loss rates in the tropical middle stratosphere, variability in surface N₂O appeared to be governed by cross-tropopause,

transport and mixing, rather than directly by the QBO. They showed evidence for a coherent influence of those dynamics on the surface N₂O seasonal cycle in the NH but not the SH.

Deleted: exchange (STE) dynamics

Deleted: in the lowermost stratosphere

Deleted: STE

Nevison *et al.* (2011) argued that cross-tropopause transport and mixing drives the N₂O seasonal minimum in both hemispheres, based on significant correlations between surface N₂O seasonal anomalies and stratospheric indices reflective of the Brewer-Dobson circulation (BDC). The BDC is a planetary-wave-driven, large-scale meridional circulation that transports ozone, greenhouse gases, and other constituents poleward and maintains the thermal structure of the stratosphere (Butchart, 2014; Minganti *et al.*, 2020). As part of this transport, the BDC brings warm, N₂O-poor air from the tropical middle and upper stratosphere into the polar lower stratosphere in the winter hemisphere (Liang *et al.*, 2008; 2009; Nevison *et al.*, 2011).

Deleted: for a STE-driven

Deleted: stratospheric temperature as well as polar vortex breakup indices

A better grasp of the controls on tropospheric N₂O variability has important implications for the interpretation of biogeochemical signals in N₂O data. If abiotic factors associated with the downward transport of N₂O-poor air from the stratosphere contribute significantly to variability, they must be disentangled from the data before inferring information about surface biogeochemistry and emissions. Understanding the influence of stratospheric variability on surface N₂O also may provide insight into anomalous changes in the AGR of CFC-11, which has a stratospheric sink similar to that of N₂O (Ray *et al.*, 2020; Ruiz *et al.*, 2021; Lickley *et al.*, 2021).

Deleted: potentially

Deleted: depleted

Deleted:

Deleted: analyzes

Deleted: interannual

Formatted: Font: (Default) +Body (Times New Roman), 12 pt

Formatted: Font: 12 pt

Formatted: Font: (Default) +Body (Times New Roman), 12 pt, Not Bold

Formatted: Font: (Default) +Body (Times New Roman), 12 pt

Formatted: Font: 12 pt

Formatted: Font: 12 pt, Italic

Formatted: Font: 12 pt

Formatted: Font: 12 pt

Formatted: Font: 12 pt, Subscript

Formatted: Font: 12 pt

Formatted: Font: 12 pt

Formatted: Font: 12 pt, Subscript

Formatted: Font: 12 pt

Formatted: Font: 12 pt, Italic

Formatted: Font: 12 pt

This paper explores the causes of variability in both the seasonal cycle and the AGR of tropospheric N₂O. It follows up on previous work by Nevison *et al.* (2011), who inferred a stratospheric influence in surface atmospheric N₂O data based entirely on correlations between interannual variations in stratospheric indices and detrended N₂O anomalies in months surrounding the seasonal N₂O minimum. In the meantime, altitude-latitude cross sections have become available from aircraft surveys that span a full seasonal cycle. In addition, advances in model development allow for explicit simulation of stratospheric N₂O tracers (Ruiz *et al.*, 2021; Liang *et al.*, 2022).

205 This study uses the NASA Goddard GEOS-5 Chemistry-Climate Model (GEOSCCM), which includes a
tagged stratospheric N₂O tracer that is transported individually in the model and distinguished from
tropospheric tracers of fresh surface emissions (Liang et al., 2022). The study also examines
atmospheric N₂O data measured by recent global airborne surveys spanning both hemispheres and
collected by the National Oceanic Atmospheric Administration (NOAA) during routine aircraft
210 monitoring in the NH. Finally, it performs an updated correlation analysis of surface N₂O anomalies
from ground-based NOAA sites against ENSO and QBO indices as well as polar lower stratospheric
temperature (PLST), which reflects the influence of the BDC.

215 The paper is organized as follows: Section 2 describes the data and methods used. Section 3 presents the
results, beginning in Section 3.1 with an examination of climatological mean seasonal cycles and
latitude-altitude cross sections of N₂O from GEOSCCM and aircraft data. Section 3.2 examines
correlations between variability in the N₂O AGR from NOAA long-term surface monitoring data,
PLST, and indices of QBO and ENSO, with the premise that significant correlations offer evidence of
causation. Section 3.3 examines correlations between PLST and variability in monthly N₂O anomalies
220 near the month of seasonal minimum. Sections 3.2 and 3.3 include parallel correlation analyses of
variability in GEOSCCM N₂O sampled at NOAA surface sites and GEOSCCM-based QBO and PLST
indices. Section 4 interprets and discusses the results. Section 5 finishes with a summary and
conclusion.

2 Methods

225 2.1 GEOSCCM with tagged stratospheric tracers

GEOSCCM was used to simulate atmospheric N₂O with geographically resolved surface emissions
from soil, ocean and anthropogenic sources, and full stratospheric chemistry with stratospheric N₂O
destruction due to photolysis and O(¹D) oxidation (Nielsen et al., 2017; Liang et al., 2022). GEOSCCM
230 has been evaluated extensively in multi-model assessments and shown to represent well the mean
atmospheric circulation, the interhemispheric exchange rate, the mean age of air in the tropical and
polar stratosphere, and the mean atmospheric lifetime of N₂O (Liang et al., 2022 and references

Moved (insertion) [1]

Deleted: . The methodology includes examination of vertic... [3]

Formatted ... [4]

Formatted ... [5]

Formatted ... [6]

Formatted ... [7]

Formatted ... [8]

Formatted ... [9]

Formatted ... [10]

Deleted: A similar correlation analysis is performed with ... [11]

Formatted ... [12]

Formatted ... [14]

Formatted ... [13]

Formatted ... [15]

Formatted ... [16]

Formatted ... [17]

Formatted ... [18]

Formatted ... [19]

Formatted ... [20]

Formatted ... [21]

Formatted ... [22]

Formatted ... [23]

Formatted ... [24]

Formatted ... [25]

Formatted ... [26]

Formatted ... [27]

Formatted ... [28]

Formatted ... [29]

Formatted ... [30]

Formatted ... [31]

Formatted ... [32]

Deleted: The GEOS-5 chemistry climate model (

Deleted:)

Formatted ... [33]

Deleted:

Formatted ... [34]

Formatted ... [35]

Formatted ... [36]

Formatted ... [37]

Formatted ... [38]

260 therein). For the current study, GEOSCCM was run at $1^\circ \times 1^\circ$ resolution with 72 vertical layers from the surface to 0.01 hPa. In addition to the standard total N_2O tracer, four additional N_2O tracers were included to track: 1) aged air from the stratosphere (N_2O_{ST}), and 2) soil, 3) ocean, and 4) anthropogenic sources freshly emitted in the troposphere. Following the approach of Liang *et al.* (2008), the tropospheric tracers become the stratospheric tracer, N_2O_{ST} , when they are transported across the tropopause, and retain that identity even when N_2O_{ST} re-enters the troposphere, thereby providing a model estimate of the stratospheric influence on tropospheric N_2O .

265 The full GEOSCCM simulation spanned 1980-2019, but this study focuses on the final 20 years from 2000-2019 for the correlation analysis between model surface N_2O anomalies and QBO and PLST. As described in detail in Liang *et al.* (2022), the GEOSCCM N_2O lifetime decreased slightly after 2000 (to 270 116 ± 2 yr in the 2010s down from 119 ± 2 yr in the 1990s) and model emissions were optimized to account for the observed change in the atmospheric N_2O growth rate. GEOSCCM temperature and QBO do not necessarily correspond to observations since both are internally generated by the GEOS general circulation model, which is free running rather than forced by a reanalysis meteorology. However, they were computed in the same way as the observed QBO and PLST indices, as described 275 below in Section 2.4.1 and 2.4.2, respectively. The GEOSCCM N_2O fields were saved as monthly means and were detrended and converted to anomalies by subtracting a deseasonalized fit to the model time series sampled at Mauna Loa.

2.2 N_2O Data

2.2.1 Surface N_2O from NOAA long-term monitoring sites

280 Surface atmospheric N_2O data were obtained from the NOAA Global Monitoring Laboratory (GML) for comparison to GEOSCCM output. NOAA has two programs that measure N_2O , Halocarbons and other Atmospheric Trace Species (HATS) (Thompson *et al.*, 2004) and the Carbon Cycle Greenhouse Gases group (CCGG) (Lan *et al.*, 2022). HATS provides *in situ* data measured every ~ 60 minutes using the Chromatograph for Atmospheric Trace Species (CATS) instruments at 5 baseline sites 285 (Barrow, Alaska; Niwot Ridge, Colorado; Mauna Loa, Hawaii; Cape Grim, Tasmania; and South Pole,

- Deleted: The model
- Deleted: chemistry mechanism
- Formatted ... [39]
- Formatted ... [40]
- Deleted: f
- Deleted: same
- Deleted: as in
- Deleted: for chlorofluorocarbons (CFCs).
- Deleted: N_2O_{ST}
- Deleted: was used to provide a model estimate of the stra ... [43]
- Formatted ... [41]
- Formatted ... [42]
- Deleted: 2000
- Formatted ... [44]
- Formatted ... [45]
- Formatted ... [46]
- Formatted ... [47]
- Formatted ... [48]
- Formatted ... [49]
- Formatted ... [50]
- Moved (insertion) [4]
- Deleted: (Liang *et al.*, 2022).The
- Formatted ... [51]
- Deleted: a
- Deleted: based on
- Formatted ... [52]
- Deleted: and the mean value at Mauna Loa is removed to ... [53]
- Deleted: The climatological seasonal cycle was analyzed ... [54]
- Deleted: from the late 1990s onward
- Formatted ... [55]
- Formatted ... [56]
- Deleted: the
- Deleted: NOAA/
- Deleted: NOAA/
- Deleted: NOAA/
- Formatted ... [57]
- Formatted ... [58]
- Formatted ... [59]
- Formatted ... [60]
- Deleted: (CATS)
- Formatted ... [61]

325 Antarctica, CCGG maintains a flask-air sampling network at ~55 widely distributed surface sampling sites, in which duplicate samples are collected about weekly and shipped to Boulder, Colorado for analysis by gas chromatography (GC) with electron capture detection and by a Tunable Infrared Laser Direct Absorption Spectroscopy (TILDAS) after August, 2019. The instruments are calibrated with a suite of standards on the WMO X2006A scale maintained by NOAA GML (Hall *et al.*, 2007). Uncertainties of the measurements (68% confidence interval) range from 0.26 to 0.43 ppb with GC-ECD and 0.16 ppb with TILDAS. The mean uncertainties in CATS GC data are 0.2 to 1.2 ppb (68% confidence interval) over most of the 2000s, with an increase in recent years as the instruments approach their lifetime.

Deleted:
Deleted: NOAA/
Formatted: Font: 12 pt

Deleted: the

Deleted: near
Formatted: Font: Bold, Font color: Auto

330 This study used the NOAA combined HATS/CCGG N₂O product from 1998-2020, which is based on monthly medians from the CATS *in situ* program (at 5 sites) and monthly means from the CCGG flask program (at 13 background sites) (<https://doi.org/10.15138/GMZ7-2Q16>; Hall *et al.*, 2007). The combined monthly data are first aggregated at the measurement program level for each sampling location. If both HATS and CCGG measure at a location, a weighted mean is calculated based on the programs' monthly uncertainties. All of the NOAA sites considered in this study, including Alert, Canada; Summit, Greenland; Mace Head, Ireland; Cape Matatula, Samoa; Palmer Station, Antarctica and the HATS baseline sites listed above, are long-standing remote sites situated away from strong local anthropogenic sources. In addition to these individual sites, global, NH and SH means are estimated from the latitude-binned and mass-weighted means of the combined monthly means for 12 background sites (Hall *et al.*, 2011).

Deleted: (<https://doi.org/10.15138/GMZ7-2Q16>)
Formatted: Line spacing: 1.5 lines

Deleted: and hemispheric

2.2.2 NOAA Empirical Background for atmospheric N₂O

345 The NOAA empirical background is a 4-dimensional (4-D) field, constructed from NOAA surface and aircraft N₂O data, which is used in North American regional inversions to represent the background concentration of atmospheric N₂O prior to the influence of continental surface fluxes (Nevison *et al.*, 2018). The 4-D field is defined daily over North America from 500-7500 m every 1000 m, from 170°-50°W every 10° longitude, and from 20-70°N every 5° latitude (or, prior to 2017, from 20-80°N every

Deleted: (EBG)
Formatted: Line spacing: 1.5 lines

Deleted: EBG

10° latitude). To construct the field, NOAA data are categorized as marine boundary layer, free troposphere or continental boundary layer, depending on the location of each sample. These three categories are treated individually as follows: For the marine boundary layer, time- and latitude-dependent reference surfaces are computed separately for the Pacific and Atlantic (Masarie and Tans, 1995, updated as described in Lan et al., 2023). For the free-troposphere, reference surfaces are created using a similar approach, with an additional “domain-filling” step informed by backward and forward trajectories for each aircraft sample collected above 3000 m AGL. For the continental boundary layer, N₂O data are detrended by subtracting the latitude and time dependent marine boundary layer reference values, where the transition from Pacific to Atlantic is represented by linear interpolation as a function of longitude across the continent. Then, a multi-year mean seasonal cycle is computed as a function of latitude, longitude, and day of year following Hammerling et al. (2012). For this study, a deseasonalized fit to the NOAA time series at Mauna Loa was used to detrend and remove the mean value (centered in the mid troposphere) of the empirical background data, thus allowing them to be collapsed into a single climatological year and presented as anomalies. The time period selected for the climatology was January 1, 2009-December 31, 2013, which roughly overlaps with the HIPPO airborne surveys described below, over a period when atmospheric N₂O was increasing by about 0.9 ppb/yr.

Deleted: 4-D

Deleted: agl

Deleted:

Deleted: using local Kriging

Deleted: (

Deleted: .

Formatted: Font: Not Italic

Formatted: Font: 12 pt, Not Bold

Formatted: Font: 12 pt, Not Bold

Formatted: Font: 12 pt, Not Bold

Formatted: Font: 12 pt, Not Bold

Formatted: Font: 12 pt

Formatted: Font: 12 pt, Not Bold

Formatted: Font: 12 pt, Not Bold

Formatted: Font: 12 pt, Not Bold

Formatted: Font: 12 pt, Not Bold

Formatted: Font: 12 pt, Not Bold

Formatted: Font: 12 pt

Deleted: QCLS atmospheric

Deleted: vertical profiling campaigns

Formatted: Portuguese (Brazil)

Formatted: Portuguese (Brazil)

Deleted: have been

Formatted: Normal, Space Before: 0 pt, After: 0 pt

Deleted: a variety of

Formatted: Portuguese (Brazil)

Deleted: vertical profiling

Deleted: s used here

Deleted: (Wofsy et al., 2011)

Deleted: specifically

2.2.3 N₂O data from global airborne surveys

Atmospheric N₂O measurements were made *in situ* with the Harvard/Aerodyne Quantum Cascade Laser Spectrometer (QCLS) on three different aircraft campaigns designed to study the atmospheric profiles of greenhouse and related gases (Wofsy et al., 2011; Stephens et al., 2018). QCLS N₂O data are retrieved at 1-Hz with 1s precision of 0.09 ppb and reproducibility with respect to the WMO N₂O scale of 0.2 ppb (Kort et al., 2011; Santoni et al., 2014) on the NOAA-2006 scale (Hall et al., 2007). The first of these campaigns, the HIAPER Pole to Pole Observations (HIPPO) project, consisted of 5 roughly month-long sets of flights centered over the central Pacific Ocean extending from the surface to the upper troposphere/lower stratosphere and nearly pole to pole (Wofsy et al., 2011). These flights were timed between January 2009 and November 2011 to create a climatological seasonal cycle. The second campaign (ORCAS), took place in January-February 2016 and focused on the Southern Ocean

south of ~35°S (Stephens et al., 2018). Most recently, the Atmospheric Tomography Mission (ATom) campaign extended nearly pole to pole over both the Pacific and Atlantic Oceans. ~~ATom consisted of 4 deployments over 3 years, with each deployment approximately 1 month long (Thompson et al., 2022).~~ QCLS N₂O was measured during the second through fourth ATom deployments in January/February 2017, September/October, 2017 and April/May 2018, respectively, but N₂O measurements are not available from the first ATom deployment in July/August 2016 due to technical problems (Gonzalez et al., 2021). For all figures presented below using QCLS N₂O, the flight track data were interpolated onto a 5 degree latitude by 50 hPa grid using the akima package in R (Akima, 1978). In addition, a deseasonalized fit to the NOAA time series at Mauna Loa was subtracted from all data, allowing them to be collapsed into a climatological year and expressed as anomalies.

2.3 Correlation analysis for surface N₂O

2.3.1 Interannual variability in the atmospheric growth rate

Interannual variability in the atmospheric growth rate of N₂O in the NOAA surface NH, SH and global time series was calculated by first removing the seasonal cycle from the monthly mean time series by computing a 12-month running average,

$$X_i = (C_{i-6} + 2 \sum_{k=i-5}^{i+5} C_k + C_{i+6})/24, \quad (1)$$

where C is the original monthly mean time series and X is the deseasonalized time series. The slope of the deseasonalized time series then was computed as a central difference,

$$S_i = 12 \frac{X_{i+1} - X_{i-1}}{2}, \quad (2)$$

where S is the centrally differenced slope and the scalar 12 converts S from units of ppb/month to ppb/yr. To account for the increasing growth rate of atmospheric N₂O, the absolute slopes S were converted to atmospheric growth rate anomalies by removing an optimal (increasing) linear fit determined by recursive least squares regression.

2.3.2 Interannual variability in the magnitude of the seasonal N₂O minimum

Formatted: Font: Not Bold

Formatted: Font: Not Bold, Italic

Formatted: Font: Not Bold

Formatted: Font: Not Bold

Formatted: Font: Not Bold, Subscript

Formatted: Font: Not Bold

Formatted: Font: Not Bold

Formatted: Font: Not Bold, Italic

Formatted: Font: Not Bold

Formatted: Font: 12 pt

Moved (insertion) [6]

Deleted: ATom consisted of four ~month-long sets of flights over 3 years, timed to create a climatological seasonal cycle (Thompson et al., 2022). QCLS N₂O was measured during ATom deployments 2-4 in January/February 2017, September/October, 2017 and April/May 2018, respectively (Gonzalez et al., 2021). (Note: technical issues interfered with the N₂O measurements on the ATom-1 deployment in July/August 2016). A

Deleted:

Deleted: has been

Deleted: since the HIPPO deployments spanned several years over a period when atmospheric N₂O was increasing by about 0.9 ppb/yr

Deleted: HIPPO data extend up to 12-14 km and provide a fuller perspective with respect to altitude than the NOAA data in Figures 4-5 of the stratospheric influence on tropospheric N₂O.

Formatted: Font: 12 pt

Formatted: Font: Bold, Font color: Auto

Deleted: surface

Deleted: at

Deleted: monitoring sites

Formatted: Line spacing: 1.5 lines

Deleted: observed over the 21st Century (Liang et al., 2022)

Moved down [2]: The atmospheric growth rate (AGR) anomalies constituted a monthly-resolved time series, which was plotted against various proxies and indices for both stratospheric influences and ENSO, as described below. Least squares linear regression correlation coefficients and p-values were computed with the assumption that a p-value < 0.05 was statistically significant at the 95% confidence level.

450 To calculate interannual anomalies in the magnitude of the seasonal minimum, the raw monthly mean
N₂O data were detrended with a 3rd-order polynomial, after which, a climatological seasonal cycle was
constructed by taking the average of the detrended data for all Januaries, Februaries, etc. This
climatological annual cycle was subtracted from the original raw data to produce a deseasonalized (but
not detrended) time series. A running 12-month annual mean of this curve was then computed as in
Equation 1, but where *C* is now the deseasonalized time series rather than the original monthly mean
time series. This analysis focused on mid and high latitude sites in the NOAA dataset. At stations with
455 gaps in the monthly data, the original 3rd order polynomial fit was used as a placeholder in the running
mean. The running mean was subtracted from the deseasonalized curve to remove the secular trend and
other low frequency variability, thus isolating the residual high frequency anomalies.

2.4 Proxies and indices for the correlation analysis

460 The computation of N₂O AGR anomalies from Section 2.3.1 created a set of monthly-resolved time
series for the SH, NH and global means. These were plotted against various proxies and indices for
both stratospheric influences and ENSO. In addition, the high frequency residuals from Section 2.3.2 at
various mid and high latitude sites were sorted by month and selected months were plotted against the
polar lower stratospheric temperature (PLST) BDC proxy described below.

2.4.1 Polar lower stratospheric temperature (PLST) as proxy for the Brewer Dobson circulation

465 Mean polar (60°-90°) lower stratospheric temperature at 100 hPa in January-March (winter) in the NH
and September-November (spring) in the SH was computed from the Modern-Era Retrospective
Analysis for Research Applications, Version 2 (MERRA-2) reanalyses (*Gelaro et al., 2017*). PLST
reflects the cumulative effect of fall/winter stratospheric downwelling due to the BDC (Holton, 2004).
The mean PLST in each hemisphere was treated as a proxy for the integrated strength of the BDC,
470 which brings warm N₂O-poor air from the middle to upper tropical stratosphere into the polar winter
lower stratosphere, with warmer PLST corresponding to stronger downwelling (*Nevison et al., 2007*;
2011). Winter months (January-March) were averaged in the NH and spring months (September-
November) in the SH to account for the later seasonal breakup of the Antarctic polar vortex compared

Formatted: Line spacing: 1.5 lines

Deleted: and

Moved down [3]: The monthly N₂O anomaly analysis was applied only to PLST BDC proxy and not to the QBO or ENSO indices, because the latter are monthly indices for which it is not straightforward to choose a representative month to correlate to the N₂O anomaly, given that the anomaly might result from the cumulative effect over multiple months. PLST in contrast has one unique value each year that can be plotted against that year's N₂O anomaly for any given month. ¶

Deleted: ¶

The high frequency residuals were sorted by month and selected months were plotted against the PLST BDC proxy described in Section 2.4.1. The months selected were those surrounding the seasonal N₂O minimum, which is the most distinct feature of the seasonal cycle at remote baseline NOAA sites and which were hypothesized, based on previous work, as most likely to be influenced by the descent of N₂O-depleted air from the stratosphere (*Nevison et al., 2011*). (Note: strong local sources can create large seasonal signals in atmospheric N₂O that dominate the stratospheric influence at some sites, e.g., those influenced by agriculture or coastal upwelling (*Lueker et al., 2003; Nevison et al., 2018; Ganesan et al., 2020*)). ¶

Moved (insertion) [2]

Deleted: atmospheric growth rate (

Deleted:)

Deleted: onstituted

Formatted: Subscript

Formatted: None, Space Before: 0 pt, After: 0 pt, Line spacing: 1.5 lines

Deleted: , which

Deleted: was

Deleted: , as described below. Least squares linear regression correlation coefficients and p-values were computed with the assumption that a p-value < 0.05 was statistically significant at the 95% confidence level. ¶

Moved (insertion) [3]

Deleted: The monthly N₂O anomaly analysis was applied only to PLST BDC proxy and not to the QBO or ENSO indices, because the latter are monthly indices for which it is not straightforward to choose a representative month to correlate to the N₂O anomaly, given that the anomaly might result from the cumulative effect over multiple months. PLST in contrast has one unique value each year that can be plotted against that year's N₂O anomaly for any given month. ¶

Deleted: winter/spring (

Formatted: Line spacing: 1.5 lines

Deleted: spring (

Deleted: depleted

Deleted: W

to the Arctic polar vortex (Nevison *et al.*, 2011). For the monthly analysis, the PLST proxy was regressed against the monthly N₂O anomaly in each of the subsequent months leading up to and encompassing the seasonal minimum in tropospheric N₂O, which occurs in summer in the NH and autumn in the SH. For the AGR analysis, the mean N₂O AGR anomaly was averaged over 12 months (considering a range of start/end months) for regression against PLST.

2.4.2 Quasi-Biennial Oscillation (QBO)

The QBO was quantified using monthly mean stratospheric zonal wind values in m/s derived from twice daily balloon radiosondes conducted by the Meteorological Service Singapore Upper Air Observatory at a station located at 1.34°N, 103.89°E (https://acd-ext.gsfc.nasa.gov/Data_services/met/qbo/QBO_Singapore_Uvals_GSFC.txt). A positive QBO indicates westerly winds and a negative QBO indicates easterly winds. A range of altitudes from 10 mb to 100 mb was considered. Since the QBO index is a monthly mean time series, it can be compared directly to the monthly mean N₂O AGR time series. However, delays are expected between the QBO and its influence on tropospheric N₂O (Strahan *et al.*, 2015; Ray *et al.*, 2020). Therefore, a range of lag times was considered spanning 6-24 months when correlating with the N₂O AGR anomalies to identify the optimal QBO altitude and lag in each hemisphere.

2.4.3 ENSO

ENSO cycles were defined using the Niño 3.4 index, which is based on sea surface temperature anomalies from 5°S to 5°N and 170° to 120°W. The Niño 3.4 index defines an El Niño event as a temperature anomaly of > 0.4 degrees C, and a La Niña event as a temperature anomaly of < -0.4°C. Monthly Niño 3.4 indices were obtained from <https://www.cpc.ncep.noaa.gov/data/indices/sstoi.indices>. Like the QBO index, Niño 3.4 is a monthly time series that can be compared directly to the monthly mean N₂O AGR time series. In the analysis presented here, a range of lag times in the Niño 3.4 index was considered spanning 0-12 months to identify the optimal lag in each hemisphere.

2.5 GEOSCCM correlation analysis

Deleted: atmospheric

Moved up [1]: The QBO is a tropical, lower stratospheric, downward-propagating zonal wind variation with an average period of ~28 months that dominates the variability of tropical lower stratospheric meteorology (Baldwin *et al.*, 2001; Butchart, 2014).

Formatted: Line spacing: 1.5 lines

Deleted: The El Niño Southern Oscillation (ENSO) index refers to the oscillation between warm (El Niño) and cold (La Niña) phases in the eastern tropical Pacific Ocean. El Niño is a periodic warming and deepening of the thermocline in the eastern tropical Pacific associated with westerly wind anomalies that excite eastward propagating downwelling equatorial Kelvin waves (McPhadden *et al.*, 1998). ...

Deleted: T

Formatted: Font: 12 pt

Deleted: , defines

Deleted: . Conversely, the index defines

Deleted: a temperature anomaly of < -0.4°C defines as a

Formatted: Font: 12 pt

Formatted: Font: 12 pt

Formatted: Font: 12 pt

Formatted: Font: 12 pt

Formatted: Font: 12 pt

Deleted: comparison

Formatted: Font: 12 pt

560 Equations 1 and 2 were applied to GEOSCCM N₂O output sampled at the coordinates of NOAA
monitoring sites to create modeled N₂O AGR time series and monthly anomalies, using both total N₂O
and N₂O_{ST}. Similarly, mean winter and spring PLST at 100 hPa was calculated for GEOSCCSM
output in the NH and SH, respectively, as described in Section 2.4.1, for each model year from 2000-
2019. Finally, a GEOSCCM monthly QBO index was calculated at a range of altitudes from 10 mb to
565 100 mb by averaging the model zonal wind component in m/s between 5°S and 5°N over each of the
240 months from 2000-2019. A correlation analysis was performed using the GEOSCCM N₂O AGR
and monthly anomaly time series regressed against GEOSCCM PLST and QBO, similar to that
described for the observed quantities in Sections 2.3-2.4. The ENSO correlation analysis was not
570 applied to GEOSCCM output because the model did not attempt to reproduce the impact of ENSO on
surface flux variability (Liang et al., 2022).

Formatted: Font: 12 pt

Deleted: (Note: t

Deleted:)

Moved up [4]: The GEOSCCM N₂O fields are detrended based on a deseasonalized fit to the model time series sampled at Mauna Loa and the mean value at Mauna Loa is removed to create the anomalies.

Deleted: ¶
GEOSCCM simulates a strong stratospheric influence on the surface N₂O seasonal cycle in both hemispheres, in which air depleted in N₂O accumulates during winter in the polar lower stratosphere and crosses the tropopause in springtime (early summer) in the NH (SH) (Figure 1). The N₂O depleted air moves downward and mixes equatorward from January to May at SH mid-to-high latitudes and from March to August at NH mid-to-high latitudes. Due to these lags in downward propagation and mixing, the surface minimum in the lower troposphere is not felt until autumn in both hemispheres (Figure 2). ¶

... [63]

Formatted

... [62]

Deleted: T

Deleted: seasonal cycle in tropospheric

Formatted: Line spacing: 1.5 lines

Deleted: loss

Formatted: Subscript

Deleted: emissions from soil, ocean and anthropogenic

Deleted: ,

Deleted: although

Deleted: (Figure 3)

Deleted: Comparison to

Deleted: data at long-term monitoring sites suggests

Deleted: Southern Hemisphere

Deleted: high northern latitud

Deleted: (Figure 3)

Deleted: ¶

3. Results

3.1 Stratospheric influence on tropospheric N₂O in model and aircraft data

575 Figure 1 shows that the GEOSCCM N₂O mean seasonal cycle at surface sites is dominated by
stratospheric air depleted in N₂O that is transported to the surface, rather than by the influence of
surface sources. However, the surface emissions tend to pull the total N₂O seasonal minimum about 1
month earlier than the N₂O_{ST} minimum at most sites. Figure 1 also shows that GEOSCCM captures the
mean observed seasonal cycle in N₂O relatively well at sites in the SH but overestimates the amplitude
of the cycle at sites in the NH, with a ~1-2 month delay in phasing relative to observations.

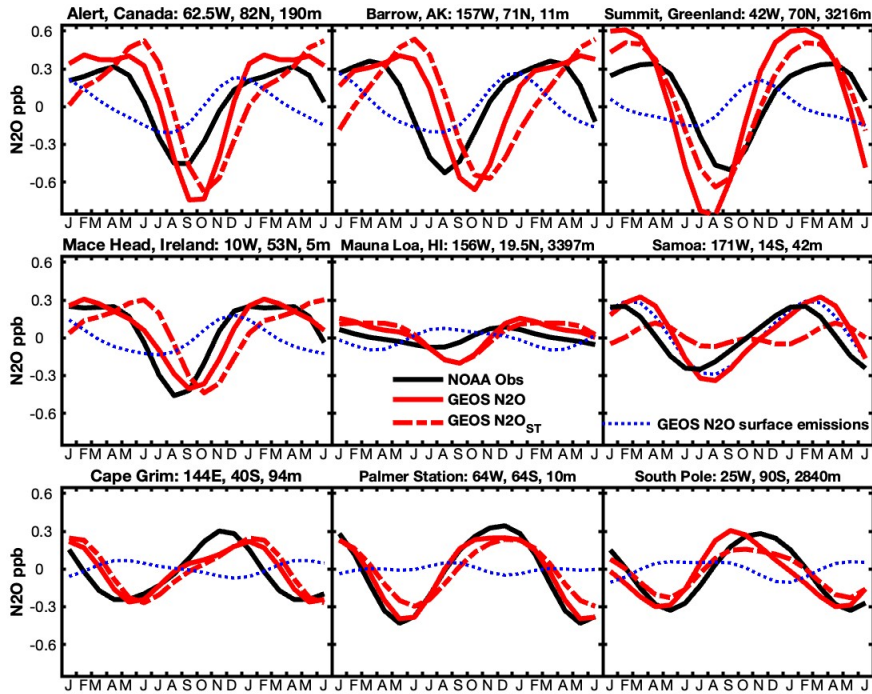
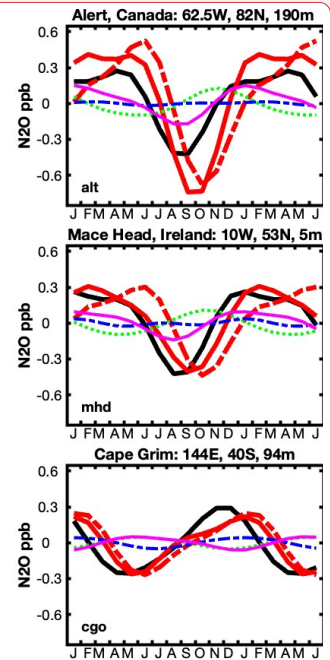


Figure 1. Detrended seasonal cycles in atmospheric N_2O modeled by GEOSCCM and compared to NOAA surface station data at 9 surface sites. Top row from left to right: Alert (Canada), Barrow (Alaska), Summit (Greenland); middle row from left to right: Mace Head (Ireland), Mauna Loa (Hawaii), Cape Matatula (Samoa); bottom row from left to right: Cape Grim (Tasmania), Palmer Station (Antarctica), South Pole (Antarctica). The black heavy line is observed N_2O from NOAA. For GEOSCCM, the total N_2O from all forcings is in red and the stratospheric tracer N_2O_{ST} is in dashed red. The dotted blue line is N_2O due to fresh surface emissions, representing the combined net influence of the natural soil, ocean, and anthropogenic atmospheric tracers.

Figure 2 provides a two-dimensional view, using zonally-averaged altitude-month contour plots at middle and high latitudes in both hemispheres, of how the signal of stratospheric air depleted in N_2O is transmitted to the surface in GEOSCCM. This N_2O -poor air accumulates during winter (starting in ~December in the NH and ~July in the SH) in the polar stratosphere, descends vertically and crosses into the troposphere in spring (March-April) in the NH and early summer (January-February) in the SH.



Deleted:

Deleted: 3

Formatted: Font: 10 pt

Formatted

... [64]

Moved (insertion) [5]

Formatted: Font: 10 pt

Deleted:

Deleted: The...red line is ...total N_2O from all forcings is in red and the , while the dashed red line is the tagged ...stratospheric tracer N_2O_{ST} .

... [65]

Formatted: Font: Bold

Moved up [5]: The black heavy line is observed N_2O .

Deleted: Surface...anomalies are shown for...ue to fresh surface emissions, representing the combined net influence of the natural soil (green)... ocean (blue)... and anthropog...

... [68]

Formatted

... [66]

Formatted

... [67]

Formatted: Font: Bold

Formatted

... [69]

Formatted: Line spacing: 1.5 lines

The SH latitude panels in Figure 2 are plotted with a 6-month shift to help visualize the later seasonal phasing of the stratospheric influence in the SH relative to the NH. After crossing into the troposphere, the N₂O-poor air continues to move downward, and also mixes equatorward, from approximately January to May at SH mid-to-high latitudes and April to October at NH mid-to-high latitudes. Due to lags in downward propagation and mixing, the modeled surface minimum in the lower troposphere does not occur until late summer to early autumn in both hemispheres (Figures 1 and 2). Supplementary Figure S1 shows a 3-dimensional view of this process in a series of 12 monthly altitude by latitude plots.

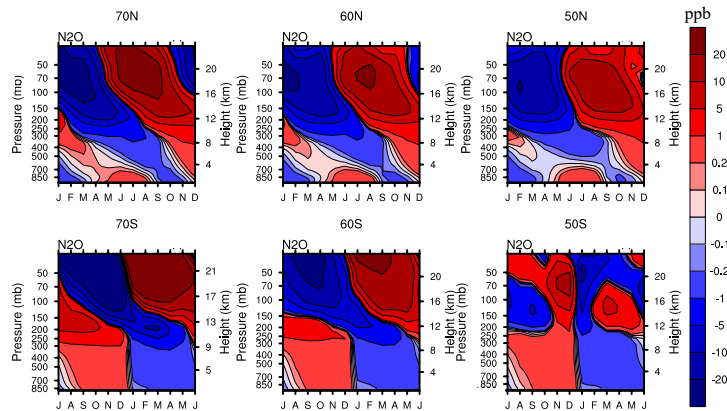


Figure 2: GEOSCCM N₂O anomalies in ppb as a function of month and altitude over a mean seasonal cycle, plotted from the surface to 30 hPa in the NH (top row) and SH (bottom row). From left to right: 10° latitude bins centered at 70°, 60° and 50°. Monthly anomalies are computed by subtracting the annual mean value at each pressure level.

Figure 3 shows that the NOAA N₂O empirical background, when organized as a series of zonally-averaged altitude-month contour plots at NH latitudes, has features similar to those simulated by GEOSCCM. Both model and observations show a signal of N₂O depletion beginning in early spring in the upper troposphere that propagates down to the surface. In both model and observations, the signal is strongest at high latitudes and weakens substantially moving equatorward. However, the NOAA data suggest a faster, more direct downward propagation of the stratospheric signal, which arrives at the

Formatted: Font: 12 pt, Not Bold

Formatted: Font: 12 pt, Not Bold

Formatted: Font: 12 pt, Not Bold

Formatted: Font: 12 pt, Not Bold

Formatted: Font: 12 pt, Not Bold

Formatted: Font: 12 pt, Not Bold

Deleted: T

Formatted: Font: (Default) +Body (Times New Roman), 12 pt

Formatted: Normal (Web), Space Before: 0.1 pt, After: 0.1 pt, Line spacing: 1.5 lines, Widow/Orphan control, Tab stops: Not at 0.39" + 0.78" + 1.17" + 1.56" + 1.94" + 2.33" + 2.72" + 3.11" + 3.5" + 3.89" + 4.28" + 4.67"

Deleted: similar

Formatted: Font: (Default) +Body (Times New Roman), 12 pt

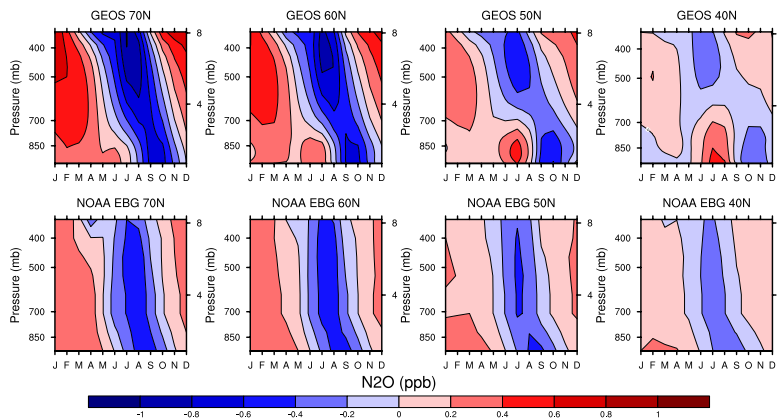
Formatted: Font: (Default) +Body (Times New Roman), 12 pt, Not Bold

Formatted: Font: (Default) +Body (Times New Roman), 12 pt

Formatted: Font: (Default) +Body (Times New Roman), 12 pt, Subscript

Formatted: Font: (Default) +Body (Times New Roman), 12 pt

700 surface in August-September, compared to September-October in GEOSCCM. As a result, the phasing of the GEOSCCM surface minimum is delayed ~1-2 months relative to the NOAA empirical background, consistent with the comparison to NOAA surface monitoring data in Figure 1.



705 **Figure 3: N₂O anomalies in ppb as a function of month and altitude over a mean seasonal cycle, plotted from the surface to 8 km (~330 hPa) in the NH for GEOSCCM (top row) and the NOAA empirical background (bottom row). From left to right: 10° latitude bins centered at 70°, 60°, 50° and 40°N. Monthly anomalies are computed by subtracting the annual mean value at each pressure level.**

710 **Figure 4 provides a further perspective on the signal of N₂O-poor stratospheric air in the NOAA empirical background. When viewed as a 12-month sequence of altitude-latitude contours, the signal originates at northern polar latitudes in the upper troposphere in late winter and early spring, descends and mixes equatorward, with a peak influence around August-September at middle to high latitudes in the NH. By late fall and winter, the signal has dissipated at the surface but is forming again in the upper**

715 **troposphere.**

Deleted: When viewed as a 12-month sequence of NH altitude vs. latitude contours, extending up to 8 km, the NOAA data indicate that the North American background signal of stratospheric depletion originates at polar latitudes in the upper troposphere in spring and is felt in the midlatitude lower troposphere by July, with a peak influence around August (Figure 4). The effect on the troposphere is strongest near the pole and weakens substantially moving equatorward. A comparison of altitude vs. month contours for GEOSCCM and NOAA suggests a faster, more direct propagation of the stratospheric signal down to the surface in the NOAA data compared to the model (Figure 5). As a result, the phasing of the GEOSCCM surface minimum is delayed ~1-2 months relative to the NOAA empirical background, consistent with the comparison to NOAA surface monitoring data in Figure 3.

Formatted: Font: (Default) +Body (Times New Roman)

Formatted: Font: (Default) +Body (Times New Roman), 12 pt

Formatted: Subscript

Formatted: Font: (Default) +Body (Times New Roman), 12 pt

Formatted: Font: (Default) +Body (Times New Roman), 12 pt

Formatted: Font: (Default) +Body (Times New Roman), 12 pt

Formatted: Font: (Default) +Body (Times New Roman), 12 pt

Formatted: Font: (Default) +Body (Times New Roman)

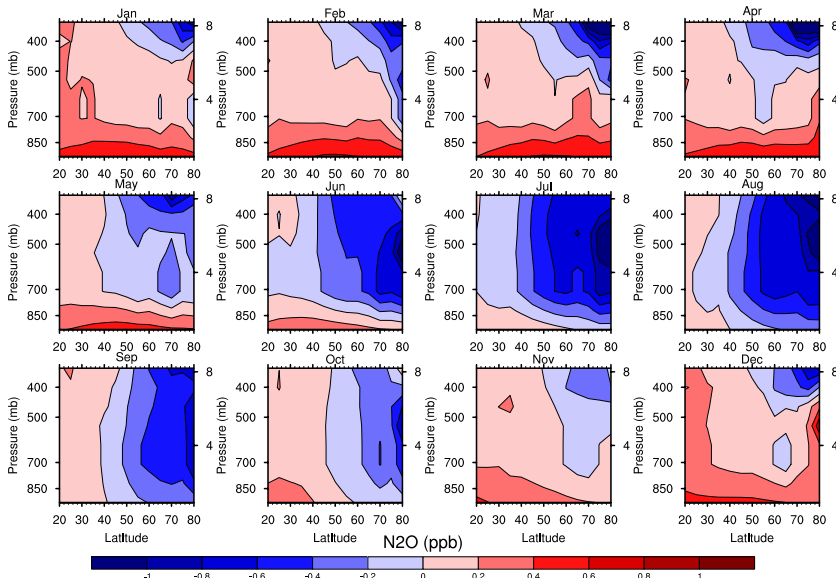


Figure 4: N_2O anomalies in the Northern Hemisphere from the NOAA empirical background, plotted in a monthly sequence of altitude vs. latitude plots extending from the surface up to 8 km (~330 hPa) and from 20°N-80°N.

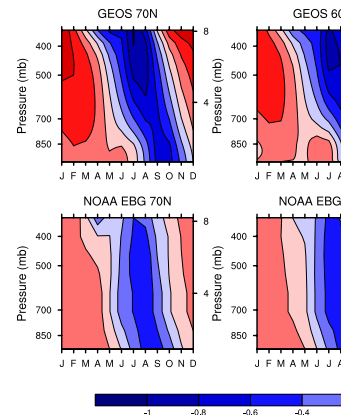
735 QCLS N_2O data from airborne surveys extend up to 14 km and thus provide a broader perspective with respect to altitude of the stratospheric influence on tropospheric N_2O . Of the 3 airborne surveys available for our analysis (HIPPO, ORCAS and ATom), HIPPO provides the most complete N_2O time series across all seasons. In Figure 5, the southbound transects from the five HIPPO deployments are detrended and arranged chronologically as altitude-latitude contour plots over an annual mean cycle.

740 These plots form a sequence with a similar movement of N_2O -poor stratospheric air from upper levels down to the surface as seen in GEOSCCM and the NOAA empirical boundary data. This progression is most readily seen in the NH in Figure 5, in which N_2O -poor air in the polar lower stratosphere has crossed the tropopause by March. By June it has descended into the middle troposphere and started moving equatorward, reaching its maximum influence at the surface in August. By October/November,

745 the stratospheric signal is no longer visible at the surface following tropospheric mixing and dilution.

Deleted: Northern hemisphere N_2O anomalies in the Northern Hemisphere from the NOAA empirical background based on NOAA regularly sampled aircraft flights... plotted in a monthly sequence of altitude vs. latitude plots extending from the surface up to ~8 km (~330 hPa) and from 20°N-80°N and from 20° to 80°N, zonally averaged over 160 to 60°W... The NOAA N_2O are detrended based on a deseasonalized fit to the observed time series sampled at the latitude, longitude and altitude of Mauna Loa. [70]

Formatted: Space After: 0 pt



Deleted: Figure 5: Northern hemisphere N_2O anomalies vs. month over a mean seasonal cycle, plotted over the height of the troposphere up to ~8 km (330 hPa), comparing GEOSCCM (top row) and the NOAA empirical background (bottom row) at 70°, 60°, 50° and 40°N zonally averaged 10° latitude bins. The GEOSCCM and NOAA N_2O fields are detrended based on their respective... [71]

Deleted: HIPPO aircraft data

Formatted: Subscript

Formatted: Line spacing: 1.5 lines

Deleted: , but with sparser temporal coverage than the NOAA empirical background

Formatted: Subscript

Deleted: The southbound transects from the five HIPPO deployments, when ... are detrended and arranged chronologically as altitude-latitude contour plots over an annual mean cycle... [72]

Formatted: Subscript

Deleted: that ... is most readily seen... easily seen in the NH in (...figure 5 6). ... in which N_2O -depleted ... or air accumulates... in the polar lower stratosphere has in January and ... crosses... the tropopause by March/April. By June it has ... By June it has descended... into the middle troposphere and started mov... [73]

This seasonal progression is also evident in a fuller dataset that also includes the ATom and northbound HIPPO transects collapsed into a climatological cycle (Supplementary Figure S2)

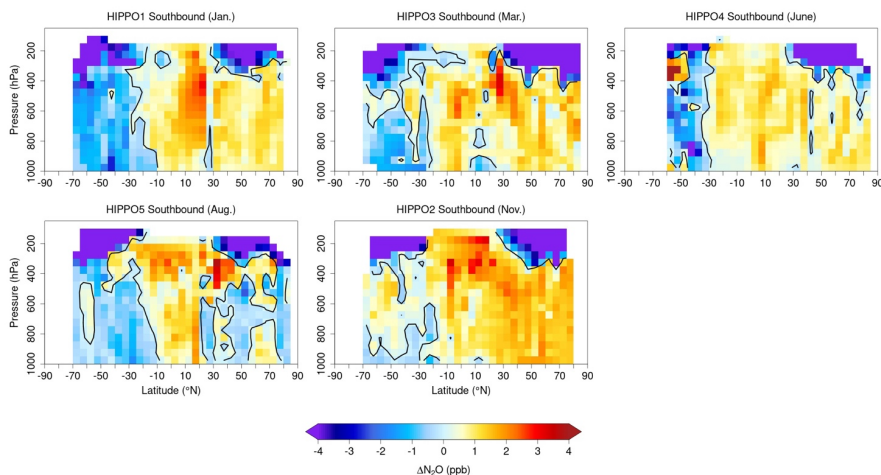


Figure 5: Sequence of five HIPPO pressure-latitude contour plots arranged to form an annual sequence; from left to right: January, March, June (top row) and August, November (bottom row). Each panel represents a north-to-south transect across latitude with vertical profiling from the surface to 14 km.

3.2 Correlation analysis of the Surface N₂O Atmospheric Growth Rate (AGR)

In this section NOAA surface N₂O AGR anomalies from 1998-2020 are plotted against polar lower stratospheric temperature (PLST) and QBO and ENSO indices, with varying lag times as described in the Methods. The analysis focuses on the NOAA global, NH, and SH mean products, with the premise that a significant correlation between the interannual variability in the N₂O AGR and one or more of the indices can be interpreted to support a causal influence of the latter on the N₂O AGR. A similar correlation analysis is performed for the GEOSCCM N₂O AGR and the model's internally-generated QBO and PLST fields, with the assumption that similarities between modeled and observed correlations may also support a causal influence.

Deleted: Notably, this seasonal progression is less apparent although still discernible in a fuller dataset that also includes the ATom and northbound HIPPO transects (Supplementary Figure 1).

Deleted: 6

Deleted: southbound

Deleted: transects

Formatted: Font: 10 pt

Formatted: Font: 10 pt

Formatted: Font: 10 pt, Bold

Formatted: Font: 10 pt

Moved up [6]: A deseasonalized fit to the NOAA time series at Mauna Loa has been subtracted from all data, since the HIPPO deployments spanned several years over a period when atmospheric N₂O was increasing by about 0.9 ppb/yr. HIPPO data extend up to 12-14 km and provide a fuller perspective with respect to altitude than the NOAA data in Figures 4-5 of the

Deleted: Flight track data were interpolated onto a 5 degree latitude by 50 hPa grid using the akima package in R (Akima, 1978). A deseasonalized fit to the NOAA time series at Mauna Loa has been subtracted from all data, since the HIPPO deployments spanned several years over a period when atmospheric N₂O was increasing by about 0.9 ppb/yr. HIPPO data extend up to 12-14 km and provide a fuller perspective with respect to altitude than the NOAA data in Figures 4-5 of the stratospheric influence on tropospheric N₂O.

Formatted: Font: 10 pt

Moved up [7]: The correlations between surface N₂O and stratospheric temperature are strongest for NOAA N₂O in January and February (austral summer), and for GEOSCCM N₂O in February and March, when N₂O is descending into its seasonal minimum.

Moved (insertion) [7]

Deleted: 3.2 Interannual variability in the seasonal N₂O minimum

In the SH, polar lower stratospheric temperature (PLST) from the previous spring is significantly negatively correlated to NOAA surface station N₂O monthly anomalies in austral summertime (January and February), when N₂O is descending into its autumn seasonal minimum. This correlation is observed at several extratropical southern NOAA sites including Cape Grim, T...

Deleted: 3

Deleted: Interannual Variability in

Deleted: of

Deleted: Surface N₂O

Formatted: Subscript

Formatted: Line spacing: 1.5 lines

Formatted: Subscript

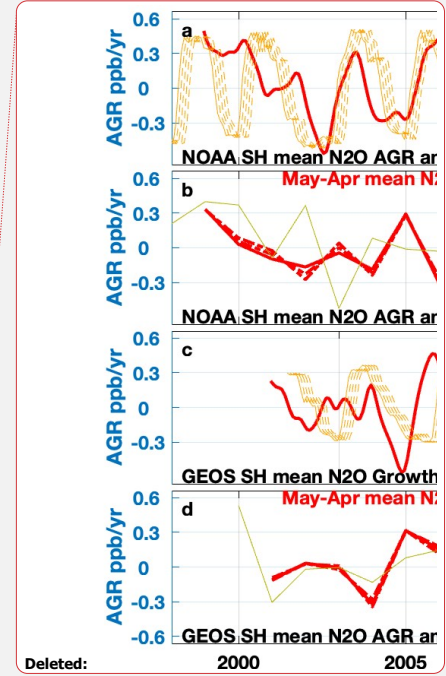
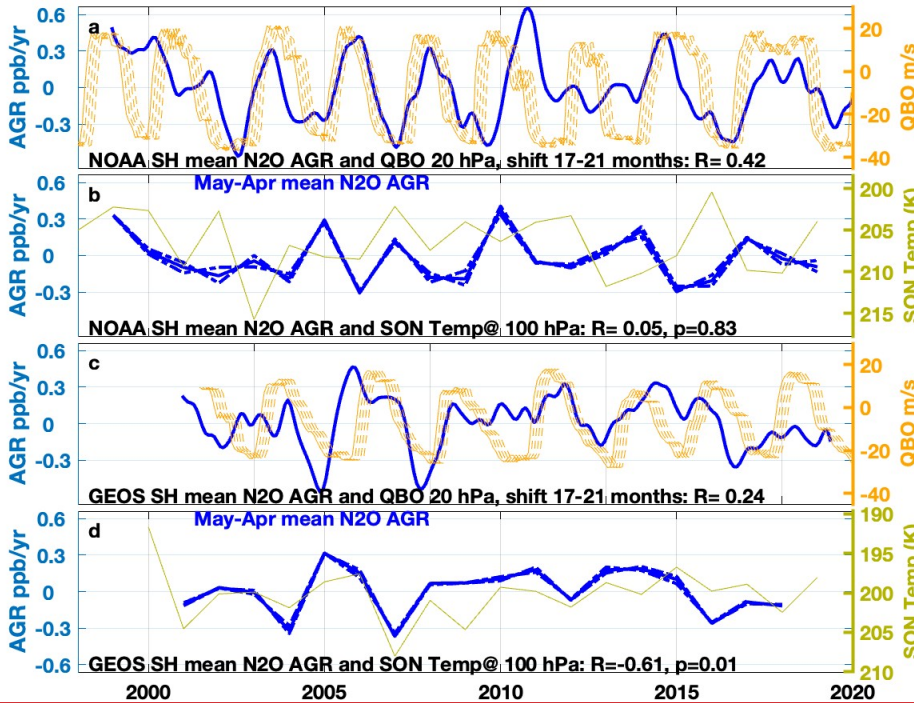
Formatted: Subscript

Formatted: Subscript

935 Figure 6a shows that in the SH the QBO index is positively correlated to the NOAA observed surface
N₂O AGR_v with an optimal correlation (R = 0.42) for QBO in the upper stratosphere at 20 hPa with a
time shift of about 19 (17-21) months relative to the N₂O time series. The correlation between
GEOSCCM QBO and the SH N₂O AGR_v is weaker (R = 0.24) but also positive in sign in the upper
stratosphere with a similar optimal shift in the GEOSCCM QBO of about 19 months (Figure 6c).

940 Spring PLST is not significantly correlated to the NOAA surface N₂O AGR in the SH (Figure 6b), but
within GEOSCCM the two are negatively correlated (Figure 6d). The correlation with PLST in
GEOSCCM occurs for the N₂O AGR averaged over a range of different 12-month intervals, with the
strongest correlation (R = -0.61) over the 12-month interval from May-April (Figure 6d).

Deleted: T
Deleted: in the SH
Deleted:
Deleted: (Figure 9a)
Deleted: in the SH
Deleted: 9



- Deleted: 9
- Deleted: (a,c) Southern hemisphere
- Deleted: (a)
- Deleted: (c)
- Deleted: red
- Deleted: red
- Deleted: (b)
- Deleted: (d)
- Deleted: 9
- Formatted: Line spacing: 1.5 lines
- Formatted: Subscript
- Deleted: is negative in sign and not significantly
- Deleted: any
- Deleted: of the weak
- Deleted: s

950 Figure 6: SH N₂O atmospheric growth rate (AGR) for (a) NOAA and (c) GEOSCCM, plotted with the QBO index at 20 hPa with a 17-21 month forward shift in the index. (b,d) SH N₂O AGR plotted with mean lower stratospheric temperature averaged over 60-90°S for September-November in the year prior to the annual label on the X axis. The AGR is averaged from monthly N₂O data over the ensuing 12 month period May-April (solid blue line), shifted plus or minus 1 month (dotted blue lines), for (b) NOAA and (d) GEOSCCM. Note: to convert to %/yr (AGR units often used in the literature) ppb/yr can be multiplied by 100/323 (~1/3), where 323 is the mean tropospheric mixing ratio of N₂O over 1998-2020.

960 In contrast to the SH, the NOAA surface N₂O AGR in the NH is significantly correlated to winter PLST (R = -0.61), with an optimal correlation for the 12-month period from July-June encompassing the January-March PLST average (Figure 7b). A similar correlation is found between the GEOSCCM PLST and NH N₂O AGR (Figure 7d). Also in contrast to the SH, the NOAA NH N₂O AGR is correlated only weakly to the QBO index at all altitudes, with a negative sign. The strongest correlation

in the NH occurs for 50 hPa QBO (R=-0.23) with a 10-14 months lag (Figure 7a). GEOSCCM predicts a **stronger** negative correlation (R = -0.47) between the GEOSCCM QBO and the NH N₂O AGR, which also is optimal around 50 hPa with 10-14 month QBO lag (Figure 7c).

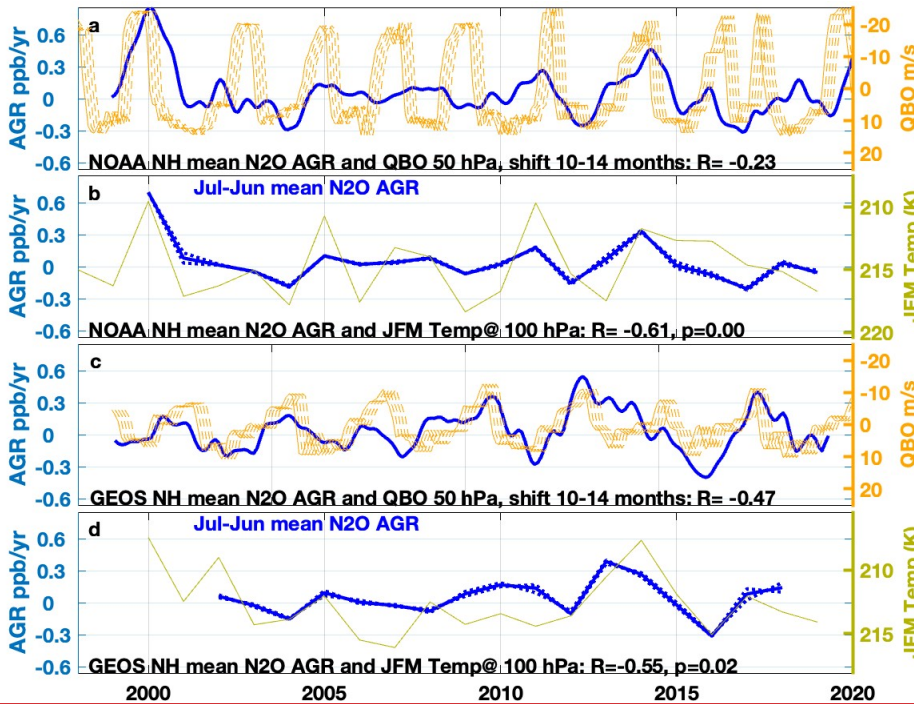


Figure 7: NH N₂O atmospheric growth rate (AGR) for (a) NOAA and (c) GEOSCCM plotted with the QBO index at 50 hPa with a 10-14 month forward shift in the index. (b,d) NH N₂O AGR plotted with mean lower stratospheric temperature averaged over 60-90°N for January-March of the year labeled on the X axis. The AGR is averaged from monthly N₂O data over the encompassing 12 month period July-June (solid blue line), shifted plus or minus 1 month (dotted blue lines), for (b) NOAA and (d) GEOSCCM.

The Niño 3.4 index is negatively correlated (R = -0.5) to the NOAA surface N₂O AGR both globally

Deleted: 10

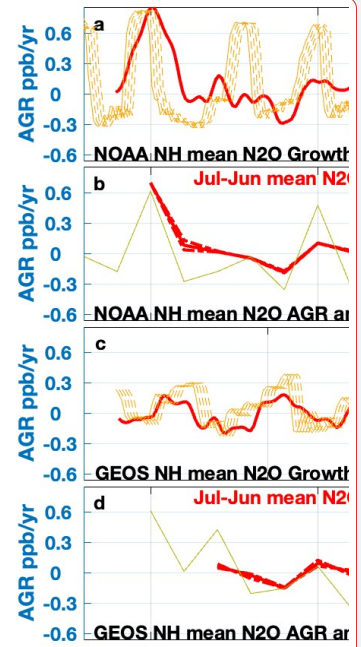
Deleted: significant

Moved (insertion) [8]

Deleted: 10

Deleted: In the NH, winter PLST

Deleted: is negatively correlated to the NOAA surface N₂O AGR (R = -0.61) with an optimal correlation for the 12 month period of July-June encompassing the January-March PLST average (Figure 10b). A similar correlation is found between the GEOSCCM (... [75])



Deleted:

Deleted: Figure 10: (a,c) Northern hemisphere N₂O atmospheric growth rate (AGR) for NOAA (a) and GEOS (c) plotted with the QBO index at 50 hPa with a 10-14 month forward shift in the index. (b,d) NH N₂O AGR plotted (... [76])

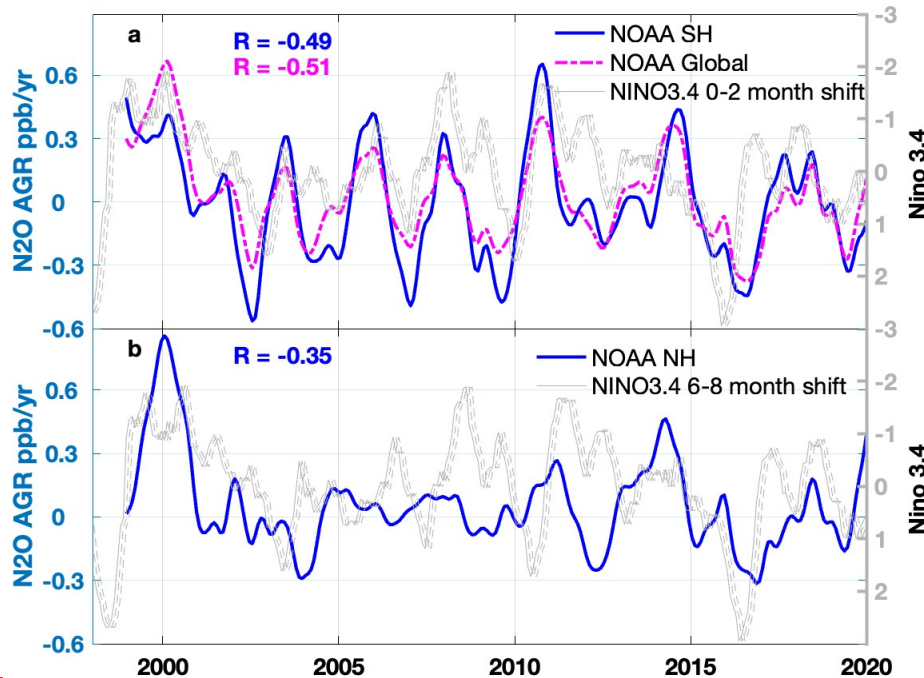
Deleted: In the SH, PLST is not significantly correlated to the surface N₂O AGR observed by NOAA, but within GEOSCCM the two are negatively correlated (Figure 9b,d). The correlation with PLST in GEOSCCM occurs for the N₂O AGR averaged over (... [77])

Moved up [8]: In the NH, winter PLST is negatively correlated to the NOAA surface N₂O AGR (R = -0.61) with an optimal correlation for the 12 month period of July-June encompassing the January-March PLST average (Figure 10b). A similar correlation is

Deleted:

Formatted: Line spacing: 1.5 lines

and in the SH, with little to no monthly lag in the index. In the NH, the correlation is weaker ($R = -0.35$) with an optimal lag of 7 months in the Niño 3.4 index relative to the NOAA N₂O AGR (Figure 8).

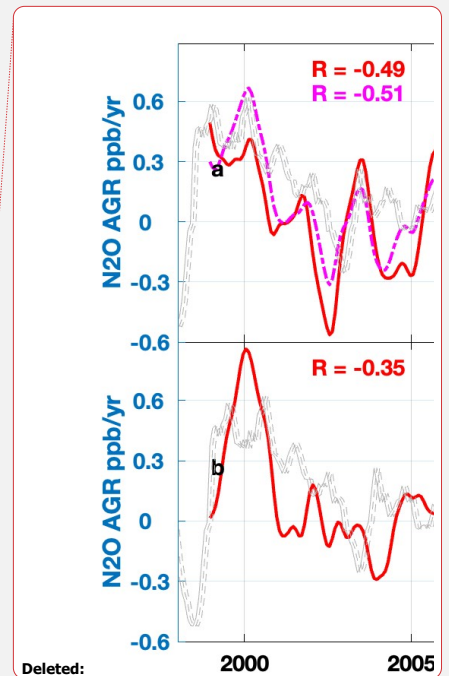


045 Figure 8: NOAA N₂O AGR plotted with the Niño3.4 index for a) SH and global mean AGR with a 0-2 month shift in the index and b) NH AGR with a 6-8 month shift in the index.

3.3 Correlation analysis of N₂O monthly anomalies

050 The N₂O monthly anomaly correlation analysis is focused solely on PLST, which has one unique value each year that can be plotted against the corresponding N₂O anomaly for any given month. The months selected for this correlation analysis were those surrounding the seasonal N₂O minimum, which is the most distinct feature of the seasonal cycle at remote mid and high latitude NOAA sites. These months

Deleted: 11



Deleted:

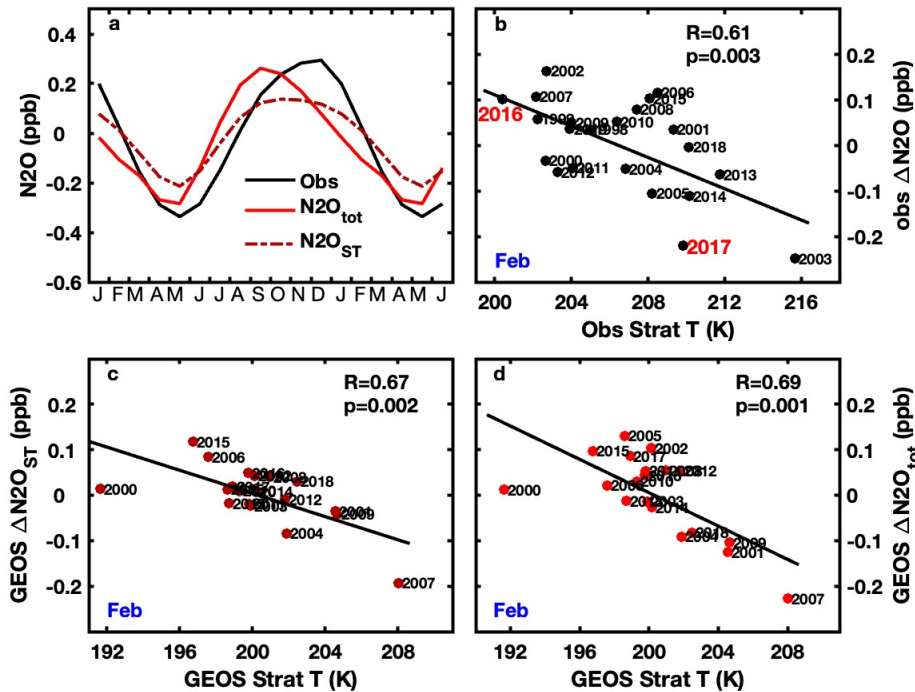
Deleted: 11

Formatted: Line spacing: 1.5 lines

were hypothesized, based on previous work, as most likely to be influenced by the descent of N₂O-poor air from the stratosphere (Nevison *et al.*, 2011). In contrast, QBO and ENSO are monthly indices for which it is not straightforward to choose a representative month to correlate to the N₂O monthly anomaly, given that the anomaly might result from the cumulative effect over multiple months.

060 Figure 9 shows that in the SH, PLST from the previous spring is significantly negatively correlated to NOAA surface station N₂O monthly anomalies in austral summertime, when N₂O is descending into its autumn seasonal minimum (Figure 9a). This correlation is observed in January and February at several extratropical southern NOAA sites including Cape Grim, Tasmania, Palmer Station, Antarctica, and
065 South Pole and is shown for February at South Pole in Figure 9b. The sign of the correlation is such that more negative surface N₂O anomalies occur during warm years, in which stronger than average descent of N₂O-poor air occurs into the polar lower stratosphere over the austral winter and spring. GEOSCCM simulates similar correlations between PLST and austral summer N₂O anomalies, both for N₂O_{ST} and total N₂O (Figure 9c,d) at these sites, although the correlations are strongest in February and March, i.e.,
070 delayed by about 1 month relative to NOAA surface observations.

Formatted: Line spacing: 1.5 lines



075 **Figure 9:** Top row shows a) South Pole mean seasonal cycle in N₂O for observed N₂O and GEOSCCM total N₂O and N₂O_{ST} and b) NOAA surface N₂O seasonal anomalies in February at South Pole spanning 1998-2020, plotted vs. mean lower stratospheric MERRA-2 temperature at 100 hPa averaged over 60-90°S over the previous spring (September-November). The labeled anomalies in 2016 and 2017 correspond to the year of the ORCAS and ATom-2 aircraft surveys, respectively. Bottom row shows GEOSCCM seasonal anomalies for c) N₂O_{ST} and d) total N₂O in February at South Pole spanning 2000-2019, plotted vs. mean GEOSCCM lower stratospheric temperature, which is sampled the same way as the MERRA-2 temperature.

080 **Figure 10**, which compares February altitude-latitude N₂O contour plots from the ORCAS and ATom airborne surveys, offers support for the observed surface correlations in Figure 9. The contour plots show more depleted N₂O values in the extratropical SH during ATom-2, which took place in February 2017 after a relatively warm spring in the Antarctic lower stratosphere (strong BDC), compared to ORCAS, which took place in January-February 2016 after a particularly cold spring (weak BDC). The right panel shows ATom-2 data over the full 65°S to 75°N latitude span, putting the stratospheric

Formatted: Font: 12 pt

Formatted: Font: 12 pt

Formatted: None, Space After: 0 pt, Line spacing: 1.5 lines, Widow/Orphan control, Tab stops: Not at 0.39" + 0.78" + 1.17" + 1.56" + 1.94" + 2.33" + 2.72" + 3.11" + 3.5" + 3.89" + 4.28" + 4.67"

Formatted: Font: 12 pt

influence coming from the southern polar stratosphere into broader perspective. The left panel extends only from 70°S to 20°S because ORCAS was confined to that region.

Formatted: Font: 12 pt

Formatted: Font: 12 pt

Formatted: Font: Bold

090

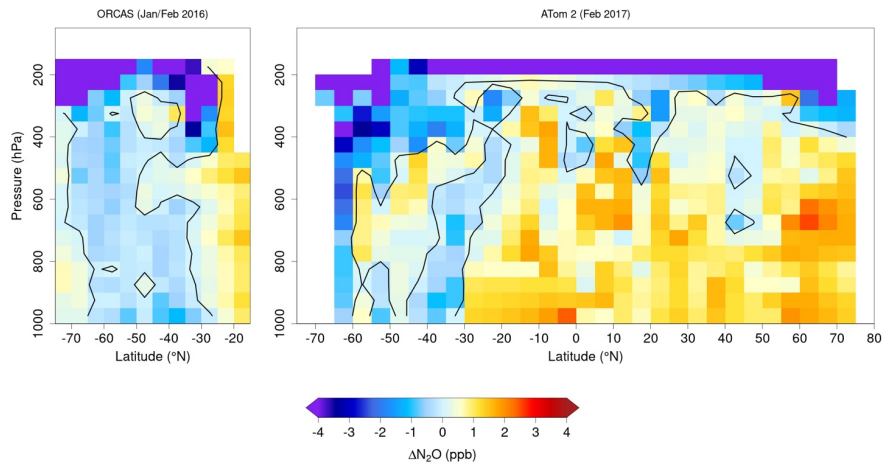


Figure 10. N₂O anomalies in ppb as a function of altitude and latitude from (left panel) ORCAS (Jan.-Feb. 2016) and (right panel) ATom-2 (Jan.-Feb. 2017).

095

In contrast to the SH, PLST in the NH from the previous winter is not correlated significantly to N₂O monthly anomalies at extratropical NOAA surface sites in any of the months surrounding the NH N₂O seasonal minimum. GEOSCCM also does not predict significant correlations between PLST and summer N₂O anomalies at most northern NOAA sites, with the exception of Mace Head, Ireland (MHD), where a negative correlation is found in July (Supplementary Figure S3).

100

4. Discussion

The atmospheric N₂O observations and model results assembled here present several new lines of evidence that the stratosphere helps drive the seasonal minimum in tropospheric N₂O and also influences its atmospheric growth rate. First, the vertical cross sections of atmospheric N₂O from

Deleted: Both t

Deleted: and the NOAA surface station and QCLS aircraft observations present

Deleted: suggest

Formatted: Subscript

Formatted: Line spacing: 1.5 lines

Deleted: Multiple lines of evidence point to this conclusion. First, vertical profile

Deleted: s

aircraft provide a broad-scale perspective, in which N₂O-poor air shows up in the winter polar lower stratosphere, crosses the tropopause around the time of polar vortex breakup, and descends downward and equatorward, reaching Earth's surface by summer or early fall. These patterns are seen in both the NOAA empirical background and in global airborne survey data (Figures 3, 4, 5). Second, GEOSCCM simulations show similar 3-dimensional patterns to those in the NOAA empirical background (Figure 4) as well as correlations between the surface N₂O AGR with internally modeled QBO and PLST indices that are similar to those found in observations (Figures 6, 7). In addition, GEOSCCM predicts correlations between February N₂O anomalies and PLST in the SH, both for total N₂O, similar to those observed, and for the explicitly resolved stratospheric N₂O tracer N₂O_{ST} (Figure 9).

The comparison of GEOSCCM output to NOAA observations, while supporting a stratospheric influence on the troposphere, also raises questions. The phasing of the GEOSCCM N₂O seasonal cycle is delayed relative to observations, especially in the NH, and the model simulates too long a delay in propagating stratospheric signals down to the surface (Figure 1.3). The rate of descent in the stratosphere has been shown to be underestimated in atmospheric models (e.g. *Brühl et al., 2007; Khosrawi et al., 2009; 2018*) and this may also be the case in the troposphere. Another issue is that the seasonality of surface N₂O emissions may not be well represented in the GEOSCCM simulation, e.g., summer soil emissions may be overestimated, leading to unrealistic surface maxima in July (*Liang et al., 2022*).

With respect to the aircraft data, the NOAA empirical background and QCLS vertical cross sections, while showing similar features, are not matched exactly for comparison. QCLS data are measured across a narrow longitude band of the flight track for any given latitude on a limited number of days, while the NOAA empirical background is shown as a monthly mean, zonally averaged across most of the western hemisphere (170°-50°W). Consequently, QCLS data are more likely to display synoptic-scale variability, such as the apparent surface source plumes over the Southern Ocean seen in Figure 10.

4.1 Correlation to stratospheric indices: signs and magnitudes

Deleted: new, big picture

Deleted: depleted

Deleted: originates

Deleted: in spring or early summer

Deleted: Second,

Deleted: PLST and QBO indices correlate significantly to the surface N₂O AGR in the NH and SH, respectively. PLST also correlates with monthly anomalies at or near the time of the seasonal minimum in the SH

Formatted: Subscript

Deleted: .

Deleted: These correlations are consistent with a stronger stratospheric influence in years with a stronger Brewer Dobson circulation and are similar to correlations found in previous studies (*Nevison et al., 2007; 2011*).

Deleted: Finally, GEOSCCM simulations with an explicitly resolved stratospheric N₂O tracer yield similar N₂O AGR correlations with internally modeled QBO and PLST indices, and show similar 3-dimensional patterns to those in the NOAA empirical background and in QCLS aircraft data, although with some differences in phasing and propagation time of the stratospheric signal to the surface.

Formatted: Space After: 3 pt

Formatted: Subscript

Formatted: Font: Italic

Formatted: Font: Italic

Formatted: Subscript

Formatted: Space After: 3 pt

Formatted: Font: Bold

Formatted: Space Before: 12 pt, After: 12 pt, Line spacing: single, Widow/Orphan control, Tab stops: Not at 0.39" + 0.78" + 1.17" + 1.56" + 1.94" + 2.33" + 2.72" + 3.11" + 3.5" + 3.89" + 4.28" + 4.67"

160 The results of the correlation analysis based on NOAA surface N₂O data are similar to those found in previous studies based on Advanced Global Atmospheric Gases Experiment (AGAGE) surface N₂O data (Prinn et al., 2000; Nevison et al., 2007; 2011). In general, these correlations are weak, in part because the variability in surface N₂O is very small compared to its mean tropospheric mixing ratio. Nevertheless, PLST in the NH correlates significantly to NOAA surface N₂O AGR anomalies (Figure 7b) and PLST in the SH correlates significantly to monthly N₂O anomalies in February near the time of the seasonal N₂O minimum (Figure 9b). The negative sign of these correlations is easily understood and consistent with more transport of warm, N₂O-poor air into the polar lower stratosphere in years with stronger BDC, with subsequent cross-tropopause transport that deepens the descent of N₂O into its seasonal minimum and slows the observed AGR of N₂O at the surface.

165

170 The reason for the positive correlation of the QBO index with the SH surface N₂O AGR (Figure 6a,c) is less obvious. A similar correlation in the SH, but not the NH, has been observed in other studies Ray et al. (2020) but not fully explained. In our analysis, the positive correlation between the QBO and the SH N₂O AGR is strongest for the QBO at 20 hPa with 17-19 months lag and then weakens with decreasing QBO altitude down to 100 hPa, with a concurrent decrease in the optimal lag, likely due to the time needed for downward propagation of QBO winds (Supplementary Figure S4). At 50 hPa, we find an optimal lag time of 10-12 months (R = +0.33), consistent with Ray et al. (2020).

175

180 Photochemical destruction of N₂O is highest when QBO winds above 30 hPa are in the westerly (positive) phase and lower altitude QBO winds are in the easterly (negative) phase. This configuration is associated with increased vertical upwelling in the tropical lower stratosphere, which transports more N₂O to its peak loss region around 32 km (Strahan et al., 2021; Ruiz et al., 2021). Thus the magnitude of QBO-associated photochemical destruction per se cannot be the main driver of the stratospheric influence on surface N₂O, since one would logically expect a negative correlation (i.e., slower growth in the troposphere due to more stratospheric N₂O loss during positive QBO). Ruiz et al. (2021) similarly

185 concluded that surface variability in N₂O is not correlated directly to the QBO-driven variability in

Formatted: Subscript

Formatted: Subscript

Formatted: Subscript

Formatted: Subscript

Formatted: Subscript

Formatted: Line spacing: 1.5 lines

Formatted: Subscript

Moved (insertion) [10]

Deleted: Like our study, Ray et al. (2020) found a positive correlation between the QBO index at 50 hPa and the NOAA surface N₂O AGR in the SH (but not the NH). Their QBO index was somewhat lower in altitude than our optimally selected altitude (20 hPa) and their optimal phase shift was somewhat less (8-12 months) than our optimal 19 month phase shift. This was likely a result of the time lag in the downward propagation of the QBO winds. O

Deleted: own correlation

Deleted: across a range of altitudes shows

Deleted: a

Deleted: in

Deleted: which the correlation

Deleted: and

Deleted: time decreases with decreasing altitude

Deleted:

Deleted: 3

Formatted: Subscript

Moved down [9]: The dynamics of the QBO, its interaction with the BDC and ultimate influence on surface N₂O are complex, as described above.

Deleted: ¶

4.1 The Brewer Dobson circulation¶

The mechanistic pathway by which the stratosphere imparts a distinct seasonal signature to surface N₂O is linked to the Brewer Dobson circulation (BDC), which transports warm, N₂O-depleted air from the middle and upper stratosphere into the polar lower stratosphere in the winter hemisphere (Holton et al., 1995; Liang et al., 2008; 2009; Nevison et al., 2011; Buchart, 2014). This wintertime descent leads to a large seasonal amplitude in the polar lower stratosphere, in which the N₂O mixing ratio reaches its minimum in spring just before the time of polar vortex break-up. N₂O-depleted air is brought into the troposphere by slow di...

Deleted: e

Deleted: anomaly

Deleted: is not

Deleted: determinant

Deleted: otherwise

Deleted: between the upper altitude QBO and the surface (... [79])

Formatted: Subscript

stratospheric loss, but rather by dynamical variations in cross tropopause fluxes of air, which are governed at least in part by the BDC.

The dynamics of the QBO, its interaction with the BDC and ultimate influence on surface N₂O are complex. However, the positive correlation of QBO, peaking at 20 hPa, with the SH N₂O AGR, could be explained in the context of *Strahan et al. (2015)*, as described in detail in the Supplementary Materials, Section S1. Briefly, the QBO has an associated meridional circulation, which transports N₂O-poor air poleward from the region of peak photochemical destruction in the tropics between about 30 hPa to 10 hPa in altitude. Paradoxically, this meridional circulation transports less N₂O-poor air toward the poles during the phase when the QBO is positive above 30 hPa. The N₂O-poor air subsequently is trapped in the Antarctic polar vortex and undergoes BDC-driven diabatic descent, in isolation from mixing with lower latitudes, arriving largely intact in the lower stratosphere and eventually at earth's surface, with a long lag time consistent with the 17-19 month lag found in Figure 9a.

4.2 Northern vs. southern hemisphere differences

In the NH, the planetary wave activity that drives the BDC is stronger due to the more variable topography and stronger land-sea contrasts. Consequently, the BDC-driven descent into the winter pole is more strongly seasonal and the NH polar vortex is less isolated (*Scaife and James, 2000, Kidston et al., 2015*), such that any signal associated with the QBO meridional circulation does not transport intact to lower altitudes (*Strahan et al., 2015*). This may explain why, for both NOAA surface stations and GEOSCCM, the NH N₂O AGR is more strongly correlated to PLST (a proxy for the BDC) than it is to the QBO, consistent with *Ruiz et al. (2021)*.

In contrast to the NH, the NOAA SH surface N₂O AGR does not correlate to PLST. This result is somewhat puzzling given the significant correlation between PLST and NOAA N₂O February anomalies at SH high latitude surface sites (Figure 9), which are supported by the ATom-2 and ORCAS data (Figure 10). It appears that the impact of the stratosphere in austral summer as tropospheric N₂O

Moved (insertion) [9]

Formatted: Subscript

Formatted: Font: Italic

Formatted: Subscript

Formatted: Subscript

Formatted: Line spacing: 1.5 lines

Deleted: , as described above.

Moved up [10]: Like our study, *Ray et al. (2020)* found a positive correlation between the QBO index at 50 hPa and the NOAA surface N₂O AGR in the SH (but not the NH). Their QBO index was somewhat lower in altitude than our optimally selected altitude (20 hPa) and their optimal phase shift was somewhat less (8-12 months) than our optimal 19 month phase shift. This was likely a result of the time lag in the downward propagation of the QBO winds. Our own correlation analysis across a range of altitudes shows a positive correlation between QBO and the SH N₂O AGR in which the correlation weakens and the optimal lag time decreases with decreasing altitude (Supplementary Figure S3). At 50 hPa, we find an optimal lag time of 10-12 months (R = 0.33), consistent with *Ray et al. (2020)*.

Deleted: 4.3 Northern vs. southern hemisphere differences

In the NH, some of the same mechanisms and interactions between the QBO and BDC occur, but they are more difficult to isolate than in the SH due to the more complex atmospheric dynamics of the NH stratosphere. The deposition of momentum from planetary scale Rossby waves propagating into the stratosphere is the fundamental driver of the BDC. *Holton and Tan (1980)* originally showed that a deep and cold northern winter polar vortex was associated with the QBO westerly phase, and a weaker and warmer vortex associated with the easterly phase. Hence, the year-to-year integrated strength of the BDC is tied to the interaction of the NH mean flow with the QBO. Further, the BDC strength and structure is also tied to meridional mixing of air. In addition to the QBO influence on the northern polar vortex, the QBO induces a meridional circula... [80]

Deleted: surface

Deleted: but does correlate to QBO

Formatted: Font: 12 pt

Formatted: Normal (Web), Space Before: 0.1 pt, After: 0.1 pt, Line spacing: 1.5 lines

Deleted: ,

Deleted: especially

Deleted: surface station

Deleted: monthly

Formatted: Font: 12 pt

Deleted: in January and February

Deleted: 7

Deleted: corroborated

Formatted: Font: 12 pt

Deleted: 8

descends into its seasonal minimum is not sufficient to influence the N₂O AGR across the whole SH over the entire year. The SH N₂O AGR results may reflect the strong preservation of the QBO signal that is ultimately transported into the troposphere, as discussed above, combined with the relatively weaker BDC in the SH and/or the interference of ENSO-driven signals discussed below.

4.3 Correlations with ENSO

The NOAA surface station N₂O AGR correlation with ENSO indices is similar in magnitude to the correlations with stratospheric indices in the SH (R = -0.49, 0-2 month phase shift) and relatively weaker in the NH (R = -0.35, 7 month optimal phase shift) (Figure 10). The correlation in the SH could in part reflect meteorological shifts in the tropical low level convergence pattern during positive ENSO (El Niño) conditions. For atmospheric gases with a positive north-south latitudinal gradient, these shifts result in a lessened influence of winds from the NH on the tropical SH and an increased influence of southeasterly winds. The NOAA Samoa site at 14°S, which strongly influences the cosine-latitude-weighted SH average, is known to be affected by these kinds of wind shifts (Prinn et al., 1992; Nevison et al., 2007). The fact that the N₂O AGR correlation with ENSO is considerably weaker in the NH than in the SH suggests a limited impact of ENSO on NH N₂O and supports the hypothesis that reduced north-to-south transport during positive ENSO contributes to the correlation observed in the SH.

The negative correlation between N₂O AGR and ENSO also may reflect a true reduction in the biogeochemical N₂O source during the positive ENSO phase, for example, due to drought over tropical land or due to reduced upwelling in the tropical ocean (Ishijima et al., 2009; Thompson et al., 2013). The most well documented biogeochemical response of N₂O to ENSO events occurs in the Eastern Tropical South Pacific (ETSP), a well known oxygen minimum zone (OMZ) and hot spot of oceanic N₂O emissions (Arévalo-Martínez, 2015; Ji et al., 2019). El Niño conditions decrease upwelling in the ETSP, thereby reducing the surface productivity, deepening the oxycline, contracting the OMZ and decreasing the N₂O sea-to-air flux (Ji et al., 2019; Babbín et al., 2015).

- Deleted: SH
- Deleted: a full
- Deleted: 12-month period
- Deleted: ¶
- Deleted: surf zone
- Formatted: Font: 12 pt
- Formatted: Font: 12 pt
- Formatted: Font: 12 pt
- Deleted: mixes into the polar region and
- Deleted: as per Strahan et al. (2015)
- Formatted: Font: (Default) +Body (Times New Roman), 12 pt
- Deleted: The fact that PLST does correlate with the SH N₂O AGR in GEOSCCM output suggests that GEOSCCM may overestimate the influence of the BDC in the SH or that the correlation may be clearer due to the lack of a competing ENSO influence in GEOSCCM. ...
- Deleted: 4
- Formatted: Line spacing: 1.5 lines
- Deleted: , e.g., at the NOAA Samoa site,
- Deleted: heighten
- Formatted: Font: 12 pt
- Deleted:
- Formatted: Font: Italic
- Deleted: ; Nevison et al., 2007).
- Deleted: El Niño phases
- Deleted: ¶
- Formatted: Font: 12 pt, English (UK)
- Formatted: Font: 12 pt

However, less than one quarter of the total N₂O budget likely comes from oceanic emissions, of which the ETSP is only one component (Yang et al., 2020; Canadell et al., 2021). This raises questions about whether a reduced ETSP source (or a strengthened source during La Niña periods) has enough leverage to control the overall N₂O AGR. Ruiz et al. (2021) removed the stratospheric influence from surface N₂O data to tease out a source of ~ 1 Tg N (about 5% of the total annual N₂O source) associated with the 2010 La Niña event, which could have come from tropical land or ocean, or some combination of both. Similarly, Kort et al. (2011) found evidence of strong episodic pulses of ~ 1 Tg N from tropical regions, based on maxima in QCLS N₂O data measured in the middle and upper troposphere during aircraft campaigns in 2009. These pulses were not tied specifically to an ENSO event but rather more generally demonstrated the strength of the tropical N₂O source.

Deleted: it is likely that

Formatted: Font: 12 pt

Formatted: Font: 12 pt

5 Summary and Conclusions

N₂O observations from aircraft provide direct evidence for a stratospheric influence on tropospheric N₂O that previously was inferred based on correlations of surface N₂O data to stratospheric indices.

Deleted: provided a testament to

Deleted: ¶

The 1 Tg N La Niña source inferred by Ruiz et al. (2021) raises the possibility that both ENSO and the stratosphere may jointly influence the N₂O AGR, in a manner that may complicate single variable correlation analyses. Consistent with this hypothesis, in our own study, a multivariate correlation of both QBO at 20 hPa with 19 month lag and the Niño 3.4 index with 0 months lag better captures the variability in the SH N₂O AGR (R = 0.61) than either index alone (R = 0.42 and -0.49, respectively).¶

Moved down [11]: Global airborne surveys provide new insights into stratospheric influences on tropospheric N₂O and advance our ability to understand surface variability in N₂O sources.

Formatted: Line spacing: 1.5 lines

Formatted: Subscript

Formatted: Subscript

Deleted: N₂O observations from these surveys support

Deleted: in

Deleted: showing

Deleted: depleted

Deleted: accumulates

Deleted: polar

Deleted: the

Deleted: summer to early-autumn period

Deleted: .

Deleted: delivered

Deleted: Stratosphere

Deleted: sphere exchange

GEOSCCM simulations corroborate the view that N₂O-poor air descends throughout the winter into the polar lower stratosphere, crosses the tropopause in spring or early summer, and descends downward and equatorward, transmitting a diluted but still coherent signal to Earth's surface in late summer to early autumn (August-September in the NH, April-May in the SH). In support of this view and consistent with previous studies, significant correlations are found between the N₂O AGR observed at long-term NOAA surface monitoring sites and either the QBO index in the SH or PLST in the NH, where PLST is a proxy for the strength of the BDC. Correlations between the N₂O AGR and ENSO indices are also significant in the SH, suggesting a joint influence of ENSO and the stratosphere on the AGR in that hemisphere. The QBO influences the rate at which N₂O is transported to and destroyed in the tropical middle to upper stratosphere, but complex atmospheric dynamics buffer how variations in the stratospheric N₂O loss rate are transmitted across the tropopause to modulate the surface N₂O AGR.

Cross-tropopause transport in polar regions is linked closely to the BDC and appears to be a more direct influence than the QBO on the N₂O AGR in the NH. In contrast, in the SH, the combination of a better-preserved QBO signal and weaker BDC may lead to a direct (albeit with a ~1.5 year lag) correlation

505 between the QBO and the SH N₂O surface AGR, consistent with current knowledge of stratospheric dynamics. To further refine our understanding of variability in tropospheric N₂O, long-term monitoring at surface and aircraft-based sites is essential and would be complemented by more global airborne surveys extending into the lower stratosphere. The latter provide new insights into stratospheric influences on tropospheric N₂O and advance our ability to interpret and quantify surface N₂O sources.

- Deleted: our
- Deleted: understanding
- Formatted: Subscript
- Moved (insertion) [11]
- Deleted: G
- Deleted:
- Deleted: understand surface variability in
- Deleted: ¶

510 Code Availability

Codes are available from the corresponding author upon request.

Data Availability

NOAA N₂O data can be obtained by contacting xin.lan@noaa.gov or through the NOAA Global Monitoring Laboratory at https://gml.noaa.gov/aftp/data/trace_gases/n2o/flask/. QCLS N₂O data are
515 openly available and archived in the Oak Ridge National Laboratory Distributed Active Archive Center (ORNL DAAC) <https://doi.org/10.3334/ORNLDAAC/1925> (ATom), and at the National Center for Atmospheric Research (NCAR) <https://doi.org/10.5065/D6SB445X> (ORCAS) and https://doi.org/10.3334/CDIAC/HIPPO_010 (HIPPO).

Author contributions

520 CDN designed and carried out the analysis and prepared the main manuscript and most of the figures. QL implemented separate stratospheric and tropospheric N₂O tracers in GEOSCCM and provided model output. PN computed QBO indices and MERRA stratospheric temperatures and provided guidance on stratospheric dynamics. BBS, RC, YG and EK provided QCLS N₂O data and BBS created contour plots of the QCLS data. XL and GD provided N₂O surface data. All authors reviewed and
525 approved the manuscript.

Competing Interests

The authors declare they have no conflicts of interest.

Acknowledgments

530 CDN and QL acknowledge support from the NASA MAPS program (award 16-MAP16-0049). The authors are grateful to Arlyn Andrews, Colm Sweeney, Bradley Hall, Ed Dlugokencky, Steve Wofsy, Bruce Daube, and many others who have made this study possible, through collection and analysis of surface station and NOAA aircraft flasks, in situ NOAA station measurements, and QCLS aircraft campaign observations. The HIPPO and ORCAS observations, and the contributions of BBS were supported by the National Center for Atmospheric Research, which is a major facility sponsored by the
535 National Science Foundation under Cooperative Agreement No. 1852977.

References

- Akima, H.: A Method of Bivariate Interpolation and Smooth Surface Fitting for Irregularly Distributed Data Points, ACM Transactions on Mathematical Software, Vol. 4, No. 2, June 1978, pp. 148-159. Copyright 1978, Association for Computing Machinery, Inc, 1978
- Arévalo-Martínez, D. L., Kock, A., Löscher, C. R., Schmitz, R. A. & Bange, H. W.: Massive nitrous oxide emissions from the tropical South Pacific Ocean. *Nat. Geosci.*, 8, 530, 2015.
- Babbin, A.R., Bianchi, D., Jayakumar, A, and Ward, B. B.: Rapid nitrous oxide cycling in the suboxic ocean, *Science*, 348, doi:10.1126/science.aaa8380, 2015.
- 550 Baldwin, M.P., Gray, L.J., Dunkerton, T.J., Hamilton, K., Haynes, P.H., Randel, W.J., Holton, J.R., Alexander, M.J., Hirota, I., Horinouchi, T., Jones, D.B.A., Kinnerson, J.S., Marquardt, C., Sato, K., Takahashi, M., The quasi-biennial oscillation, *Reviews of Geophysics*, 39(2), 179-229, 2001.
- Bouwman, A.F. and Taylor, J.A.: Testing high-resolution nitrous oxide emission estimates against observations using an atmospheric transport model, *Global Biogeochem. Cy.*, 10, 307-318, 1996.
- 555 Bouwman, A.F., van der Hoek, K.W., and Olivier, J.G.J.: Uncertainties in the global source distribution of nitrous oxide, *J. Geophys. Res.*, 100, 2785-2800, 1995.
- [Brühl, C., Steil, B., Stiller, G., Funke, B., and Jöckel, P.: Nitrogen compounds and ozone in the stratosphere: comparison of MIPAS satellite data with the chemistry climate model ECHAM5/MESy1, *Atmos. Chem. Phys.*, 7, 5585–5598, <https://doi.org/10.5194/acp-7-5585-2007>.](https://doi.org/10.5194/acp-7-5585-2007)
- 560 Butchart, N.: Reviews of Geophysics The Brewer-Dobson circulation, *Rev. Geophys.*, 52, 157–184. <https://doi.org/10.1002/2013RG000448>, 2014.
- Canadell, J. G., P. M. S. Monteiro, M. H. Costa, L. Cotrim da Cunha, P. M. Cox, A. V. Eliseev, S. Henson, M. Ishii, S. Jaccard, C. Koven, A. Lohila, P. K. Patra, S. Piao, J. Rogelj, S. Syampungani, S. Zaehle, K. Zickfeld, 2021, Global Carbon and other Biogeochemical Cycles and Feedbacks. In: *Climate Change 2021: The Physical Science Basis. Contribution of Working Group I to the Sixth Assessment Report of the Intergovernmental Panel on Climate Change (Masson-Delmotte, V., P. Zhai, A. Pirani, S. L. Connors, C. Péan, S. Berger, N. Caud, Y. Chen, L. Goldfarb, M. I. Gomis, M. Huang, K. Leitzell, E. Lonnoy, J.B.R. Matthews, T. K. Maycock, T. Waterfield, O. Yelekçi, R. Yu and B. Zhou (eds.)). Cambridge University Press. In Press.*
- 565 Earth Systems Research Laboratory, Multivariate ENSO Index (MEI). NOAA (2017).
- Elkins, J.W, and Dutton, G.S.: Nitrous oxide and sulfur hexafluoride (in 'State of the Climate in 2008'), *Bull. Amer. Meteor. Soc.*, 90, S38-S39, 2009.
- Forster, P., Ramaswamy, V., Artaxo, P., Berntsen, T., Betts, R., Fahey, D.W., Haywood, J., Lean, J., Lowe, D.C., Myhre, G., Nganga, J., Prinn, R., Raga, G., Schulz, M. and Van Dorland, R.: Changes in
- 575 Atmospheric Constituents and in Radiative Forcing. In: *Climate Change 2007: The Physical Science Basis. Contribution of Working Group I to the Fourth Assessment Report of the Intergovernmental Panel on Climate Change. Cambridge University Press Cambridge, United Kingdom and New York, NY, USA, 2007.*
- Gonzalez, Y., Commane, R., Manninen, E., Daube, B.C., Schiferl, L., McManus, J.B., McKain, K,
- 580 Hints, E.J., Elkins, J.W., Montzka, S.A., Impact of stratospheric air and surface emissions on

Formatted: Normal (Web), Automatically adjust right indent when grid is defined, Space Before: 0.1 pt, After: 0.1 pt, Line spacing: 1.5 lines, Widow/Orphan control, Adjust space between Latin and Asian text, Adjust space between Asian text and numbers, Tab stops: Not at 0.39" + 0.78" + 1.17" + 1.56" + 1.94" + 2.33" + 2.72" + 3.11" + 3.5" + 3.89" + 4.28" + 4.67"

Formatted: Font color: Auto

Deleted: Glatthor, N., von Clarmann, T., Fischer, H., Funke, B., Grabowski, U., Hoepfner, M., Kellmann, S., Kiefer, M., Linden, A., Milz, M., Steck, T., Stiller, G.P., Mengistu Tsidu, G., Wang, D.-Y.: Mixing processes during the Antarctic vortex split in September-October 2002 as inferred from source gas and ozone distributions from ENVISAT-MIPAS, *J. Atmos. Sci.*, 62(3), 787-800, 2005.

- tropospheric nitrous oxide during ATom, Atmospheric Chemistry and Physics Discussions, <https://doi.org/10.5194/acp-2021-167>, 2021.
- 590 Gurney, K. R., Law, R.M., Denning, A.S., Rayner, P.J., Pak, B.C., Baker, D.F., Bousquet, P.,
Bruhwiler, L., Chen, Y.-H., Ciais, P., Fung, I.Y., Heimann, M., John, J., Maki, T., Maksyutov, S.,
Peylin, P., Prather, M., Taguchi, S.: Transcom 3 inversion intercomparison: Model mean results for the
estimation of seasonal carbon sources and sinks, *Global Biogeochem. Cycles*, 18, GB1010,
doi:10.1029/2003GB002111, 2004.
- 595 Hall, B. D., Dutton, G.S., and Elkins, J. W.: The NOAA nitrous oxide standard scale for atmospheric
observations, *J. Geophys. Res.*, 112, D09305, doi:10.1029/2006JD007954, 2007.
- Hall, B. D., Dutton, G. S., Mondeel, D. J., Nance, J. D., Rigby, M., Butler, J. H., Moore, F. L., Hurst, D.
F. and Elkins, J. W.: Improving measurements of SF₆ for the study of atmospheric transport and
emissions, *Atmos. Meas. Tech.*, 4, 2441-2451, doi: 10.5194/amt-4-2441-2011, 2011.
- 600 Hammerling, D. M., Michalak, A. M., Kawa, S. R.: Mapping of CO₂ at High Spatiotemporal Resolution
using Satellite Observations: Global Distributions from OCO-2, *Journal of Geophysical Research*, 117,
D06306, doi:10.1029/2011JD017015, 2012.
- Hirsch, A.I., Michalak, A.M., Bruhwiler, L.M., Peters, W., Dlugokencky, E.J. and Tans, P.P.: Inverse
modeling estimates of the global nitrous oxide surface flux from 1998-2001, *Global Biogeochem. Cy.*,
20, GB1008, doi:10.1029/2004GB002443, 2006.
- 605 Holton, J.R., Haynes, P.H., McIntyre, M.E., Douglass, A.R., Rood, R.B. and Pfister, L.: Stratosphere-
troposphere exchange, *Rev. Geophys.*, 33(4), 403-439, 1995.
[Holton, J.: An Introduction to Dynamic Meteorology, no. v. 1 in An Introduction to Dynamic Meteorology, Elsevier Science, available at: <https://books.google.be/books?id=fhW5oDv3EPsC> \(last access: 28 October 2020\), 2004.](#)
- Huang, J., Golombek, A., Prinn, R., Weiss, R., Fraser, P., Simmonds, P., Dlugokencky, E.J., Hall, B.,
610 Elkins, J., Steele, P., Langenfelds, R., Krummel, P., Dutton, G., and Porter, L.: Estimation of regional
emissions of nitrous oxide from 1997 to 2005 using multinet network measurements, a chemical transport
model, and an inverse method, *J. Geophys. Res.* 113, D17313, doi:10.1029/2007JD009381, 2008.
- Ishijima, K., Patra, P.K., Takigawa, M., Machida, T., Matsueda, H., Sawa, Y., Steele, L.P., Krummel,
P.B., Langenfelds, R.L., Aoki, S. and Nakazawa, T.: The stratospheric influence on the seasonal cycle
615 of nitrous oxide in the troposphere as deduced from aircraft observations and model simulations, *J.*
Geophys. Res., 115, D20308, doi:10.1029/2009JD013322, 2010.
- Ji, Q., Babbin, A.R., Jayakumar, A., Oleynik, S. and Ward, BB.: 2015: Nitrous oxide production by
nitrification and denitrification in the Eastern Tropical South Pacific oxygen minimum zone.
Geophysical Research Letters, 42(24), 10,755–10,764, doi:10.1002/2015gl066853.
- 620 Ji, Q. et al.: Investigating the effect of El Niño on nitrous oxide distribution in the eastern tropical South
Pacific. *Biogeosciences*, 16(9), 2079–2093, doi:10.5194/bg-16-2079-2019, 2019.
- Jiang, X, Ku, W.L., Shia, R.-L., Li, Q., Elkins, J.W., Prinn, R.G., Yung, Y.L.: Seasonal cycle of N₂O:
Analysis of data, *Global Biogeochem. Cy.*, 21, GB1006, doi:10.1029/2006GB002691, 2007.
- 625 Jin, X. and Gruber, N.: Offsetting the radiative benefit of ocean iron fertilization by enhancing N₂O
emissions, *Geophys. Res. Lett.* 30(24), 2249, 2003.
- Jin, X., Najjar, R.G., Louanchi, F., and Doney, S.C.: A modeling study of the seasonal oxygen budget
of the global ocean, *J. Geophys. Res.*, 112, C05017, doi:10.1029/2006JC003731, 2007.

Formatted: Normal (Web), Space Before: 0.1 pt, After: 0.1 pt

Formatted: Font color: Auto

630 Kalnay, E., Kanamitsu, M., Kistler, R., Collins, W., Deaven, D., Gandin, L., Iredell, M., Saha, S.,
 White, G., Woollen, J., Zhu, Y., Leetmaa, A., Reynolds, R., Chelliah, M., Ebisuzaki, W., Higgins, W.,
 Janowiak, J., Mo, K.C., Ropelewski, C., Wang, J., Jenne, R., Joseph, D.: The NMC/NCAR 40-year
 reanalysis project, *B. Am. Meteorol. Soc.*, 77, 437– 471, 1996.

635 [Khosrawi, F., Kirner, O., Stiller, G., Höpfner, M., Santee, M. L., Kellmann, S., and Braesicke, P.:
 Comparison of ECHAM5/MESy Atmospheric Chemistry \(EMAC\) simulations of the Arctic winter
 2009/2010 and 2010/2011 with Envisat/MIPAS and Aura/MLS observations, *Atmos. Chem. Phys.*, 18,
 8873–8892, <https://doi.org/10.5194/acp-18-8873-2018>, 2018.](#)

640 [Khosrawi, F., Müller, R., Urban, J., Proffitt, M. H., Stiller, G., Kiefer, M., Lossow, S., Kinnison, D.,
 Olschewski, F., Riese, M., and Murtagh, D.: Assessment of the interannual variability and influence of
 the QBO and upwelling on tracer–tracer distributions of N₂O and O₃ in the tropical lower stratosphere,
Atmos. Chem. Phys., 13, 3619–3641, <https://doi.org/10.5194/acp-13-3619-2013>,
 2013.](#)

645 [M., and Murtagh, D.: Assessment of the interannual variability and influence of the QBO and upwelling on tracer–tracer
 distributions of N₂O and O₃ in the tropical lower stratosphere, *Atmos. Chem. Phys.*, 13, 3619–3641,
<https://doi.org/10.5194/acp-13-3619-2013>.](#)

[Kidston, J., Scaife, A., Hardiman, S. et al. Stratospheric influence on tropospheric jet streams, storm tracks and surface
 weather. *Nature Geosci* 8, 433–440 \(2015\). <https://doi.org/10.1038/ngeo2424>.](#)

Kort, E. A., Patra, P. K., Ishijima, K., Daube, B. C., Jiménez, R., Elkins, J.W., Hurst, D., Moore, F. L.,
 Sweeney, C. and Wofsy, S. C.: Tropospheric distribution and variability of N₂O: Evidence for strong
 tropical emissions, *Geophys. Res. Lett.*, 38, L15806, doi:10.1029/2011GL047612, 2011.

650 Kroeze, C., Mosier, A. and Bouwman, L.: Closing the global N₂O budget: A retrospective analysis
 1500-1994, *Global Biogeochemical Cycles*, 13, 1-8, 1999.

Lambert, A., Read, W. G., Livesey, N. J., Santee, M.L., Manney, G.L., Froidevaux, L., Wu, D.L.,
 Schwartz, M.J., Pumphrey, H.C., Jimenez, C., Nedoluha, G.E., Cofield, R.E., Cuddy, D.T., Daffer,
 W.H., Drouin, B.J., Fuller, R.A., Jarnot, R.F., Knosp, B.W., Pickett, H.M., Perun, V.S., Snyder, W.V.,
 Stek, P.C., Thurstans, R.P., Wagner, P.A., Waters, J.W., Jucks, K.W., Toon, G.C., Stachnik, R.A.,
 655 Bernath, P.F., Boone, C.D., Walker, K.A., Urban, J., Murtagh, D., Elkins, J.W., Atlas, E.: Validation of
 the Aura Microwave LihPa Sounder middle atmosphere water vapor and nitrous oxide measurements, *J.
 Geophys. Res.*, 112, D24S36, doi:10.1029/2007JD008724, 2007.

Lan, X., Dlugokencky, E.J., Mund, J.W., Crotwell, A.M., Crotwell, M.J., Moglia, E., Madronich, M.,
 Neff, D. and Thoning, K.W.: Atmospheric Nitrous Oxide Dry Air Mole Fractions from the NOAA
 660 GML Carbon Cycle Cooperative Global Air Sampling Network, 1997-2021, Version: 2022-11-21,
<https://doi.org/10.15138/53g1-x417>, 2022.

Lan, X., Tans, P., Thoning, K., & NOAA Global Monitoring Laboratory. (2023). NOAA Greenhouse
 Gas Marine Boundary Layer Reference - N₂O. (Data set). NOAA GML.
<https://doi.org/10.15138/83W5-DK71>.

665 Liang, Q., Stolarski, R.S., Douglass, A.R., Newman, P.A. and Nielsen, J.E.: Evaluation of emissions
 and transport of CFCs using surface observations and their seasonal cycles and the GEOS CCM

Formatted: Font: (Default) +Body (Times New Roman), 12 pt

Formatted: Normal (Web), Space Before: 0.1 pt, After: 0.1 pt, Tab stops: Not at 0.39" + 0.78" + 1.17" + 1.56" + 1.94" + 2.33" + 2.72" + 3.11" + 3.5" + 3.89" + 4.28" + 4.67"

Formatted: Font: (Default) +Body (Times New Roman), Font color: Auto

Deleted: Khosrawi, F., Mueller, R. Proffitt, M. H., Urban, J., Murtagh, D., Ruhnke, R. Grooß, J.-U. and Nakajima, H.: Seasonal cycle of averages of nitrous oxide and ozone in the Northern and Southern Hemisphere polar, midlatitude, and tropical regions derived from ILAS/ILAS-II and Odin/SMR observations, *J. Geophys. Res.*, 113, D18305, doi:10.1029/2007JD009556, 2008.

Formatted: Line spacing: 1.5 lines

Formatted: Normal (Web), Automatically adjust right indent when grid is defined, Space Before: 0.1 pt, After: 0.1 pt, Line spacing: 1.5 lines, Widow/Orphan control, Adjust space between Latin and Asian text, Adjust space between Asian text and numbers

Formatted: Font color: Auto

- simulation with emissions-based forcing, *J. Geophys. Res.*, 113, D14302, doi:10.1029/2007JD009617, 2008.
- 675 Liang, Q., Douglass, A.R., Duncan, B.N., Stolarski, R.S. and Witte, J.C.: The governing processes and timescales of stratosphere-to-troposphere transport and its contribution to ozone in the Arctic troposphere, *Atmos. Chem. Phys.*, 9, 3011-3025, 2009.
- Liang, Q., Nevison, C., Dlugokencky, E., Hall, B. D., & Dutton, G.: 3-D atmospheric modeling of the global budget of N₂O and its isotopologues for 1980–2019: The impact of anthropogenic emissions. *Global Biogeochemical Cycles*, 36, e2021GB007202. <https://doi.org/10.1029/2021GB007202>, 2022.
- 680 Lickley, M., Solomon, S., Kinnison, D., Krummel, P., Mühle, J., O’Doherty, S., et al.: Quantifying the imprints of stratospheric contributions to interhemispheric differences in tropospheric CFC-11, CFC-12, and N₂O abundances. *Geophysical Research Letters*, 48, e2021GL093700. <https://doi.org/10.1029/2021GL093700>, 2021.
- 685 Lovenduski, N.S., Gruber, N., Doney, S.C., and Lima, I.D.: Enhanced CO₂ outgassing in the Southern Ocean from a positive phase of the Southern Annular Mode, *Glob. Biogeochem. Cycles* 21, GB2026, doi:10.1029/2006GB002900, 2007.
- Lueker, T.J., Walker, S.J., Vollmer, M.K., Keeling, R.F., Nevison, C.D. and Weiss, R.F.: Coastal upwelling air-sea fluxes revealed in atmospheric observations of O₂/N₂, CO₂ and N₂O, *Geophys. Res. Lett.*, 30, 1292, 2003.
- MacFarling Meure, C., Etheridge, D. M., Trudinger, C. M., Steele, L. P., Langenfelds, R. L., van Ommen, T., Smith, A. and Elkins, J. W.: Law Dome CO₂, CH₄, and N₂O ice core records extended to 2000 years BP, *Geophys. Res. Lett.*, 33, L14810, doi:10.1029/2006GL026152, 2006.
- 695 Mahowald, N. M., Rasch, P. J., Eaton, B. E., Whittlestone, S. and Prinn, R. G.: Transport of radon-222 to the remote troposphere using the Model of Atmospheric Transport and Chemistry and assimilated winds from ECMWF and the National Center for Environmental Prediction/NCAR, *J. Geophys. Res.*, 102, 28139–28151, 1997.
- Masarie, K. A. and Tans, P.P.: Extension and integration of atmospheric carbon dioxide data into a globally consistent measurement record, *Journal of Geophysical Research-Atmospheres*, 100, D6, 11593-11610, 1995.
- 700 McPhaden, M. J., et al.: The tropical ocean-global atmosphere observing system: A decade of progress, *J. Geophys. Res.*, 103, 14,169–14,240, doi:10.1029/97JC02906, 1998.
- Minganti, D., Chabrilat, S., Christophe, Y., Errera, Q., Abalos, M., Prignon, M., Kinnison, D. E., and Mahieu, E.: Climatological impact of the Brewer–Dobson circulation on the N₂O budget in WACCM, a chemical reanalysis and a CTM driven by four dynamical reanalyses, *Atmos. Chem. Phys.*, 20, 12609– 12631, <https://doi.org/10.5194/acp-20-12609-2020>, 2020.
- 705 Minganti, D., Chabrilat, S., Errera, Q., Prignon, M., Kinnison, D. E., Garcia, R. R., et al. (2022). Evaluation of the N₂O rate of change to understand the stratospheric Brewer-Dobson circulation in a Chemistry-Climate Model. *Journal of Geophysical Research: Atmospheres*, 127, e2021JD036390. <https://doi.org/10.1029/2021JD036390>,
- 710 Mosier, A.R., Duxbury, J.M., Freney, J.R., Heinemeyer, O. and Minami, K.: Assessing and mitigating N₂O emissions from agricultural soils, *Climatic Change*, 40, 7-38, 2000.

Formatted: Line spacing: 1.5 lines

Formatted: English (US)

Formatted: Normal (Web), Space Before: 0.1 pt, After: 0.1 pt, Line spacing: 1.5 lines

Formatted: Font color: Auto

- Naqvi, S.W.A., Jayakumar, D.A., Narvekar, P.V., Naik, H., Sarma, V.V.S.S., D'Sousa, W., Joseph, S., and George, M.D.: Increased marine production of N₂O due to intensifying anoxia on the Indian continental shelf, *Nature*, 408, 346-349, 2000.
- 715 Nash, E.R., Newman, P.A., Rosenfield, J.E., and Schoeberl, M.R.: An objective determination of the polar vortex using Ertel's potential vorticity, *J. Geophys. Res.*, 101, 9471-9478, 1996.
- National Oceanic Atmospheric Administration (NOAA) Global Monitoring Division, Interactive Data Visualization, <https://www.esrl.noaa.gov/gmd/dv/iadv/>, accessed April 6, 2021.
- Nevison, C.D., Weiss, R.F. and Erickson III, D.J.: Global Oceanic Nitrous Oxide Emissions, *J. Geophys. Res.*, 100, 15,809-15,820, 1995.
- 720 Nevison, C.D., Kinnison, D.E. and Weiss, R.F.: Stratospheric Influence on the tropospheric seasonal cycles of nitrous oxide and chlorofluorocarbons, *Geophys. Res. Lett.* 31(20), L20103, doi:10.1029/2004GL020398, 2004.
- Nevison, C.D., Keeling, R.F., Weiss, R.F., Popp, B.N., Jin, X., Fraser, P.J., Porter, L.W. and Hess, P.G.: Southern Ocean ventilation inferred from seasonal cycles of atmospheric N₂O and O₂/N₂ at Cape Grim, 725 Tasmania, *Tellus*, 57B, 218-229, 2005.
- Nevison, C. D., Mahowald, N. M., Weiss, R.F. and Prinn, R.G.: Interannual and seasonal variability in atmospheric N₂O, *Global Biogeochem. Cy.*, 21, GB3017, doi:10.1029/2006GB002755, 2007.
- Nevison, C.D., Dlugokencky, E., Dutton, G., Elkins, J.W., Fraser, P., Hall, B., Krummel, P.B., Langenfelds, R.L., O'Doherty, S., Prinn, R.G., Steele, L.P., Weiss, R.F.: Exploring causes of interannual variability in the seasonal cycles of 730 tropospheric nitrous oxide, *Atmospheric Chemistry and Physics*, 11, doi:10.5194/acp-11-1-2011, 1-18, 2011.
- Nevison, C., Andrews, A., Thoning, K., Dlugokencky, E., Sweeney, C., Miller, S., et al.: Nitrous oxide emissions estimated with the CarbonTracker-Lagrange North American regional inversion framework. *Global Biogeochemical Cycles*, 32. <https://doi.org/10.1002/2017GB005759>, 2018.
- Newman, P.: The Quasi-biennial Oscillation (QBO). Retrieved from [https://acd- 735 ext.gsfc.nasa.gov/Data_services/met/qbo/qbo.html](https://acd-ext.gsfc.nasa.gov/Data_services/met/qbo/qbo.html), 2020.
- Nielsen, J.E., Pawson, S., Molod, A., Auer, B., da Silva, A.M., Douglass, A.R., et al.: Chemical mechanisms and their applications in the Goddard Earth Observing System (GEOS) Earth system model, *Journal of Advances in Modeling Earth Systems*, 9(8), 3019-3044, doi:10.1002/2017MS001011, 2017.
- 740 Olivier, J.G.J., Van Aardenne, J.A., Dentener, F., Ganzeveld, L. and Peters, W.: Recent trends in global greenhouse gas emissions: regional trends and spatial distribution of key sources. In: *Non-CO₂ Greenhouse Gases (NCGG-4)*, van Amstel, A. (coord.), page 325-330. Millpress, Rotterdam, 2005.
- Park, S., et al.: Trends and seasonal cycles in the isotopic composition of nitrous oxide since 1940, *Nature Geoscience*, 5, 261-265, 2012.
- 745 Plumb, R. A.: Stratospheric transport, *J. Meteorol. Soc. Jpn.*, 80, 793-809, 2002.
- Prather, M. Hsu, J., J., DeLuca, N.M., Jackman, C.H., Oman, L.D., Douglass, A.R., Fleming, E.L., Strahan, S.E., Steenrod, S.D., Sovde, O.A., Isaksen, I.S.A., Froidevaux, L., Funke, B.: Measuring and modeling the lifetime of nitrous oxide including its variability, *J. Geophys. Res. Atmos.*, 120, doi:10.1002/2015JD023267, 2015.
- 750 Prinn, R.G., Weiss, R.F., Fraser, P.J., Simmonds, P.G., Cunnold, D.M., Alyea, F.N., O'Doherty, S., Salameh, P., Miller, B.R., Huang, J., Wang, R.H.J., Hartley, D.E., Harth, C., Steele, L.P., Sturrock, G.,

- Midgley, P.M. and McCulloch, A.: A history of chemically and radiatively important gases in air deduced from ALE/GAGE/AGAGE, *J. Geophys. Res.*, 105 (D14), 17751-17792, 2000.
- 755 Ravishankara A. R., Daniel, J. S. and Portmann, R. W.: Nitrous Oxide (N₂O): The dominant ozone depleting substance emitted in the 21st century, *Science*, 326,123-125, doi: 10.1126/science.1176985, 2009.
- Ray, E. A., Portmann, R. W., Yu, P., Daniel, J., Montzka, S. A., Dutton, G. S., et al.: The influence of the stratospheric Quasi-Biennial Oscillation on trace gas levels at the Earth's surface. *Nature Geoscience*, 13(1), 22–27. <https://doi.org/10.1038/s41561-019-0507-3>, 2020.
- 760 Ruiz, D.J., Prather, M.J., Strahan, S.E., Thompson, R.L., Froidevaux, L., and Steenrod, S.D.: How atmospheric chemistry and transport drive surface variability of N₂O and CFC-11, *J. Geophys. Res.*, 2021.
- Santoni, G. W., Daube, B. C., Kort, E. A., Jiménez, R., Park, S., Pittman, J. V., Gottlieb, E., Xiang, B., Zahniser, M. S., Nelson, D. D., McManus, J. B., Peischl, J., Ryerson, T. B., Holloway, J. S., Andrews, 765 A. E., Sweeney, C., Hall, B., Hints, E. J., Moore, F. L., Elkins, J. W., Hurst, D. F., Stephens, B. B., Bent, J., and Wofsy, S. C.: Evaluation of the airborne quantum cascade laser spectrometer (QCLS) measurements of the carbon and greenhouse gas suite – CO₂, CH₄, N₂O, and CO – during the CalNex and HIPPO campaigns, *Atmos. Meas. Tech.*, 7, 1509–1526, <https://doi.org/10.5194/amt-7-1509-2014>, 2014.
- 770 Sokal, R.R. and Rohlf, F.J.: *Biometry*, 859 pp., W.H. Freeman, New York, 1981.
- [Scaife, A.A. and James, I.N. \(2000\), Response of the stratosphere to interannual variability of tropospheric planetary waves. Q.J.R. Meteorol. Soc., 126: 275- 297. https://doi.org/10.1002/qj.49712656214.](https://doi.org/10.1002/qj.49712656214)
- Stephens, B.: ORCAS Merge Products. Version 1.0, <https://doi.org/10.5065/D6SB445X>, accessed 13 Jul 2020, 2017.
- Stephens, B. B., Long, M. C., Keeling, R. F., Kort, E. A., Sweeney, C., Apel, E. C., Atlas, E. L., Beaton, S., Bent, J. D., 775 Blake, N. J., Bresch, J. F., Casey, J., Daube, B. C., Diao, M., Diaz, E., Dierssen, H., Donets, V., Gao, B.-C., Gierach, M., Green, R., Haag, J., Hayman, M., Hills, A. J., Hoecker-Martínez, M. S., Honomichl, S. B., Hornbrook, R. S., Jensen, J. B., Li, R.-R., McCubbin, I., McKain, K., Morgan, E. J., Nolte, S., Powers, J. G., Rainwater, B., Randolph, K., Reeves, M., Schauffler, S. M., Smith, K., Smith, M., Stith, J., Stossmeister, G., Toohey, D. W., and Watt, A. S.: The O₂/N₂ Ratio and CO₂ Airborne Southern Ocean Study, *B. Am. Meteorol. Soc.*, 99, 381–402, <https://doi.org/10.1175/BAMS-D-16-0206.1>, 780 2018.
- [Shepherd, T. G.: Transport in the middle atmosphere. J. Meteorol. Soc. Jpn. Ser. II, 85, 165–191, 2007. Tian, H., Xu, R., Canadell, J.G. et al. A comprehensive quantification of global nitrous oxide sources and sinks. Nature 586, 248\2013256 \(2020\). https://doi.org/10.1038/s41586-020-2780-0.](https://doi.org/10.1002/qj.49712656214)
- 785 Stohl, A.: A 1-year Lagrangian “climatology” of airstreams in the Northern Hemisphere troposphere and lowermost stratosphere, *J. Geophys. Res.*, 106(D7), 7263–7279, 2001.
- Strahan, S. E., Oman, L.D., Douglass, A.R. and Coy, L.: Modulation of Antarctic vortex composition by the quasi-biennial oscillation, *Geophys. Res. Lett.*, 42, 4216–4223, doi:10.1002/2015GL063759, 2015.
- Thompson, R.L., Dlugokencky, E., Chevallier, F., Ciais, P., Dutton, G., Langenfelds, R.L., Prinn, R.G.,

Formatted: Normal (Web), Space Before: 0.1 pt, After: 0.1 pt

Formatted: Font color: Auto

790 Weiss, R.F., Tohjima, Y., O’Doherty, S., Krummel, P.B., Fraser, P., and Steele, L.P.: Interannual
 variability in tropospheric nitrous oxide, 2013, *Geophys. Res. Lett.*, 40, 4426-4431,
 doi:10.1002/grl.50721, 2013.

Thompson, R. L., Patra, P. K., Ishijima, K., Saikawa, E., Corazza, M., Karstens, U., et al.: TransCom
 N₂O model inter-comparison-Part 1: Assessing the influence of transport and surface fluxes on
 795 tropospheric N₂O variability, *Atmospheric Chemistry and Physics*, 14(8), 4349–4368.
<https://doi.org/10.5194/acp-14-4349-2014>

~~Thompson, R. L., Ishijima, K., Saikawa, E., Corazza, M., Karstens, U., Patra, P. K., Bergamaschi, P., Chevallier, F.,
 Dlugokencky, E., Prinn, R. G., Weiss, R. F., O’Doherty, S., Fraser, P. J., Steele, L. P., Krummel, P. B., Vermeulen, A.,
 Tohjima, Y., Jordan, A., Haszpra, L., Steinbacher, M., Van der Laan, S., Aalto, T., Meinhardt, F., Popa, M. E., Moncrieff,
 800 J., and P. Bousquet: TransCom N₂O model inter-comparison, Part II: Atmospheric inversion estimates of N₂O emissions,
Atmos. Chem. Phys. Discuss., 14, 5271–5321, doi:10.5194/acpd-14-5271-2014, 2014b.~~

Thompson, R.L., Lassaletta, L., Patra, P.K., Wilson, C., Wells, K.C., Gressent, A., Koffi, E.N.,
 Chipperfield, M.P., Winiwarter, W., Davidson, E.A., Tian, H. and Canadell, J.G.: Acceleration of global
 N₂O emissions seen from two decades of atmospheric inversion, *Nature Climate Change*,
 805 <https://doi.org/10.1038/s41558-019-0613-7>, 2019.

Thompson, T.M., Elkins, J.W., Hall, B., Dutton, G.S., Swanson, T.H., Butler, J.H., Cummings, S.O.,
 Fisher, D.A.: Halocarbons and other Atmospheric Trace Species, in: Schnell, R.C., A.-M. Buggle and
 R.M. Rosson (Eds.), *Climate Diagnostics Laboratory Summary Report #27, 2002-2003*, US
 Department of Commerce, National Oceanic and Atmospheric Administration, Boulder, Colorado,
 810 2004.

Thompson, C.R., Wofsy, S.C., Prather, M.J., Newman, P.A., Hanisco, T.F., Ryerson, T.B., Fahey,
 D.W., Apel, E.C., Brock, C.A., Brune, W.H. et al.: The NASA Atmospheric Tomography (ATom)
 mission: Imaging the chemistry of the global atmosphere, *Bulletin of the American Meteorological
 Society*, 103 (3): E761–E790. DOI: <http://dx.doi.org/10.1175/bams-d-20-0315.1>, 2022.

815 Tian, H., Xu, R., Canadell, J.G., Thompson, R.L., Winiwarter, W., Suntharalingam, P., Davidson, E.A., Ciais, P., et al.: A
 comprehensive quantification of global nitrous oxide sources and sinks, *Nature*, 586, 248-255.
<https://doi.org/10.1038/s41586-020-2780-0>, 2020.

Volk, C.M., Elkins, J.W., Fahey, D., Dutton, G., Gilligan, J., Lowenstein, M., Podolske, J., Chan, K.,
 and Gunson, M.: Evaluation of source gas lifetimes from stratospheric observations, *J. Geophys. Res.*,
 820 102(D21), 25,543-25,564, 1997.

Waugh, D.W., Randel, W.J., Pawson, S., Newman, P.A. and Nash, E.R.: Persistence of the lower
 stratospheric polar vortices, *J. Geophys. Res.*, 104 (D22), 27,191-27,201, 1999.

Weiss, R.F.: The temporal and spatial distribution of tropospheric nitrous oxide, *J. Geophys. Res.* 86,
 7185-7195, 1981.

825 Wofsy, S. C., the HIPPO Science Team and Cooperating Modellers and Satellite Teams: HIAPER Pole-
 to-Pole Observations (HIPPO): Fine grained, global scale measurements for determining rates for
 transport, surface emissions, and removal of climatically important atmospheric gases and aerosols,
Phil. Trans. of the Royal Society A, 369(1943), doi:10.1098/rsta.2010.0313, 2073-2086, 2011.

Deleted: ¶

Formatted: Font: (Default) +Body (Times New Roman), 10 pt

Formatted: Space Before: 0 pt, After: 0 pt, Line spacing: 1.5 lines

Formatted: Automatically adjust right indent when grid is defined, Widow/Orphan control, Adjust space between Latin and Asian text, Adjust space between Asian text and numbers, Tab stops: Not at 0.39" + 0.78" + 1.17" + 1.56" + 1.94" + 2.33" + 2.72" + 3.11" + 3.5" + 3.89" + 4.28" + 4.67"

- 830 Wofsy, S., Afshar, S., Allen, H., Apel, E., Asher, E., Barletta, B., Bent, J., Bian, H., Biggs, B., Blake, D., and et al.: ATom: Merged Atmospheric Chemistry, Trace Gases, and Aerosols, <https://doi.org/10.3334/ORNLDAAC/1581>, accessed 13 Jul 2020, 2018.
- Wofsy, S., Daube, B., Jimenez, R., Kort, E., Pittman, J., Park, S., Commane, R., Xiang, B., Santoni, G., Jacob, D., and et al.: HIPPO Merged 10-Second Meteorology, Atmospheric Chemistry, and Aerosol
- 835 Data. Version 1.0, https://doi.org/10.3334/CDIAC/HIPPO_010, accessed 13 Jul 2020, 2017.
- WMO Greenhouse Gas Bulletin No. 14, https://library.wmo.int/doc_num.php?explnum_id=5455, 2018.
- Yang, S. et al.: Global reconstruction reduces the uncertainty of oceanic nitrous oxide emissions and reveals a vigorous seasonal cycle, *Proceedings of the National Academy of Sciences*, 117(22), 11954–
- 840 11960, doi:10.1073/pnas.1921914117, 2020.

Page 1: [1] Deleted Cynthia Nevison 2/28/24 1:29:00 PM

Page 1: [2] Deleted Cynthia Nevison 2/28/24 1:34:00 PM

Page 5: [3] Deleted Cynthia Nevison 2/28/24 5:02:00 PM

Page 5: [4] Formatted Cynthia Nevison 3/11/24 10:42:00 AM

Font: (Default) +Body (Times New Roman), 12 pt

Page 5: [5] Formatted Cynthia Nevison 3/11/24 10:42:00 AM

Font: 12 pt

Page 5: [6] Formatted Cynthia Nevison 3/11/24 10:42:00 AM

Font: 12 pt

Page 5: [7] Formatted Cynthia Nevison 3/11/24 10:42:00 AM

Font: 12 pt

Page 5: [8] Formatted Cynthia Nevison 3/11/24 10:42:00 AM

Font: 12 pt

Page 5: [9] Formatted Cynthia Nevison 3/11/24 10:42:00 AM

Font: 12 pt

Page 5: [10] Formatted Cynthia Nevison 3/11/24 10:42:00 AM

Font: 12 pt

Page 5: [11] Deleted Cynthia Nevison 2/27/24 3:47:00 PM

Page 5: [12] Formatted Cynthia Nevison 3/11/24 10:42:00 AM

Font: (Default) +Body (Times New Roman), 12 pt

Page 5: [13] Formatted Cynthia Nevison 3/11/24 10:42:00 AM

Normal (Web), Space Before: 0.1 pt, After: 0.1 pt

Page 5: [14] Formatted Cynthia Nevison 3/11/24 10:42:00 AM

Font: 12 pt

Page 5: [15] Formatted Cynthia Nevison 3/11/24 10:42:00 AM

Font: 12 pt

Page 5: [16] Formatted Cynthia Nevison 3/11/24 10:42:00 AM

Font: 12 pt

Page 5: [17] Formatted Cynthia Nevison 3/11/24 10:42:00 AM

Font: 12 pt

Page 5: [18] Formatted Cynthia Nevison 3/11/24 10:42:00 AM

Font: 12 pt

Page 5: [19] Formatted Cynthia Nevison 3/11/24 10:42:00 AM

Font: 12 pt, Subscript

▲ Page 5: [20] Formatted Cynthia Nevison 3/11/24 10:42:00 AM

Font: 12 pt

▲ Page 5: [21] Formatted Cynthia Nevison 3/11/24 10:42:00 AM

Font: 12 pt

▲ Page 5: [22] Formatted Cynthia Nevison 3/11/24 10:42:00 AM

Font: 12 pt, Subscript

▲ Page 5: [23] Formatted Cynthia Nevison 3/11/24 10:42:00 AM

Font: 12 pt

▲ Page 5: [24] Formatted Cynthia Nevison 3/11/24 10:42:00 AM

Font: 12 pt

▲ Page 5: [25] Formatted Cynthia Nevison 3/11/24 10:42:00 AM

Font: 12 pt

▲ Page 5: [26] Formatted Cynthia Nevison 3/11/24 10:42:00 AM

Font: 12 pt

▲ Page 5: [27] Formatted Cynthia Nevison 3/11/24 10:42:00 AM

Font: 12 pt

▲ Page 5: [28] Formatted Cynthia Nevison 3/11/24 10:42:00 AM

Font: 12 pt

▲ Page 5: [29] Formatted Cynthia Nevison 3/11/24 10:42:00 AM

Font: 12 pt

▲ Page 5: [30] Formatted Cynthia Nevison 3/11/24 10:42:00 AM

Font: 12 pt

▲ Page 5: [31] Formatted Cynthia Nevison 3/11/24 10:42:00 AM

Font: 12 pt, Bold

▲ Page 5: [32] Formatted Cynthia Nevison 3/12/24 4:12:00 PM

Font: 12 pt

▲ Page 5: [33] Formatted Cynthia Nevison 3/1/24 6:09:00 PM

Font: (Default) +Headings (Times New Roman), 12 pt, Not Bold

▲ Page 5: [34] Formatted Cynthia Nevison 3/1/24 6:09:00 PM

Font: (Default) +Headings (Times New Roman), 12 pt, Not Bold

▲ Page 5: [35] Formatted Cynthia Nevison 3/1/24 6:09:00 PM

Font: (Default) +Headings (Times New Roman), 12 pt, Not Bold, Subscript

▲ Page 5: [36] Formatted Cynthia Nevison 3/1/24 6:09:00 PM

Font: (Default) +Headings (Times New Roman), 12 pt, Not Bold

▲ Page 5: [37] Formatted Cynthia Nevison 3/1/24 6:09:00 PM

Font: (Default) +Headings (Times New Roman), 12 pt, Not Bold, Italic

▲ Page 5: [38] Formatted Cynthia Nevison 3/1/24 6:09:00 PM

Font: (Default) +Headings (Times New Roman), 12 pt, Not Bold

▲

Page 6: [39] Formatted Cynthia Nevison 3/1/24 6:09:00 PM

Font: (Default) +Headings (Times New Roman), 12 pt, Not Bold, Subscript

Page 6: [40] Formatted Cynthia Nevison 3/1/24 6:09:00 PM

Font: (Default) +Headings (Times New Roman), 12 pt, Not Bold

Page 6: [41] Formatted Cynthia Nevison 3/7/24 1:31:00 PM

Font: (Default) +Headings (Times New Roman), 12 pt, Not Bold, Subscript

Page 6: [42] Formatted Cynthia Nevison 3/1/24 6:09:00 PM

Font: (Default) +Headings (Times New Roman), 12 pt, Not Bold

Page 6: [43] Deleted Cynthia Nevison 2/28/24 3:38:00 PM

x

Page 6: [44] Formatted Cynthia Nevison 3/1/24 6:09:00 PM

Font: (Default) +Headings (Times New Roman), 12 pt, Not Bold

Page 6: [45] Formatted Cynthia Nevison 3/1/24 6:13:00 PM

Left, Line spacing: 1.5 lines

Page 6: [46] Formatted Cynthia Nevison 3/1/24 6:09:00 PM

Font: (Default) +Headings (Times New Roman), 12 pt, Not Bold

Page 6: [47] Formatted Cynthia Nevison 3/1/24 6:09:00 PM

Font: (Default) +Headings (Times New Roman), 12 pt, Not Bold

Page 6: [48] Formatted Cynthia Nevison 3/1/24 6:09:00 PM

Font: (Default) +Headings (Times New Roman), 12 pt, Not Bold

Page 6: [49] Formatted Cynthia Nevison 3/1/24 6:09:00 PM

Font: (Default) +Headings (Times New Roman), 12 pt, Not Bold

Page 6: [50] Formatted Cynthia Nevison 3/1/24 6:09:00 PM

Font: (Default) +Headings (Times New Roman), 12 pt, Not Bold

Page 6: [51] Formatted Cynthia Nevison 3/1/24 6:09:00 PM

Font: (Default) +Headings (Times New Roman), 12 pt, Not Bold

Page 6: [52] Formatted Cynthia Nevison 3/1/24 6:09:00 PM

Font: (Default) +Headings (Times New Roman), 12 pt, Not Bold

Page 6: [53] Deleted Cynthia Nevison 3/7/24 1:40:00 PM

x

Page 6: [54] Deleted Cynthia Nevison 2/29/24 2:23:00 PM

Page 6: [55] Formatted Cynthia Nevison 3/11/24 10:41:00 AM

Font: 12 pt

Page 6: [56] Formatted Cynthia Nevison 3/11/24 10:42:00 AM

Normal (Web), Space Before: 0.1 pt, After: 0.1 pt, Line spacing: 1.5 lines, Widow/Orphan control, Tab stops: Not at 0.39" + 0.78" + 1.17" + 1.56" + 1.94" + 2.33" + 2.72" + 3.11" + 3.5" + 3.89" + 4.28" + 4.67"

Page 6: [57] Formatted Cynthia Nevison 3/11/24 10:41:00 AM

Font: 12 pt, *Italic*

Page 6: [58] Formatted Cynthia Nevison 3/11/24 10:41:00 AM

Font: 12 pt

Page 6: [59] Formatted Cynthia Nevison 3/11/24 10:41:00 AM

Font: 12 pt, *Italic*

Page 6: [60] Formatted Cynthia Nevison 3/11/24 10:41:00 AM

Font: 12 pt

Page 6: [61] Formatted Cynthia Nevison 3/11/24 10:41:00 AM

Font: 12 pt, Not Bold

Page 12: [62] Formatted Cynthia Nevison 3/2/24 2:04:00 PM

Space Before: 12 pt, After: 12 pt, No widow/orphan control, Tab stops: 0.39", Left + 0.78", Left + 1.17", Left + 1.56", Left + 1.94", Left + 2.33", Left + 2.72", Left + 3.11", Left + 3.5", Left + 3.89", Left + 4.28", Left + 4.67", Left

Page 12: [63] Deleted Cynthia Nevison 3/2/24 2:04:00 PM

Page 13: [64] Formatted Cynthia Nevison 3/7/24 4:53:00 PM

Font: 10 pt, **Bold**

Page 13: [64] Formatted Cynthia Nevison 3/7/24 4:53:00 PM

Font: 10 pt, **Bold**

Page 13: [64] Formatted Cynthia Nevison 3/7/24 4:53:00 PM

Font: 10 pt, **Bold**

Page 13: [65] Deleted Cynthia Nevison 3/2/24 1:14:00 PM

Page 13: [65] Deleted Cynthia Nevison 3/2/24 1:14:00 PM

Page 13: [65] Deleted Cynthia Nevison 3/2/24 1:14:00 PM

Page 13: [65] Deleted Cynthia Nevison 3/2/24 1:14:00 PM

Page 13: [66] Formatted Cynthia Nevison 3/11/24 10:38:00 AM

Font: **Bold**

Page 13: [66] Formatted Cynthia Nevison 3/11/24 10:38:00 AM

Font: **Bold**

Page 13: [67] Formatted Cynthia Nevison 3/11/24 10:38:00 AM

Font: 10 pt, *Subscript*

Page 13: [67] Formatted Cynthia Nevison 3/11/24 10:38:00 AM

Font: 10 pt, *Subscript*

Page 13: [68] Deleted Cynthia Nevison 3/2/24 1:12:00 PM

Page 13: [68] Deleted Cynthia Nevison 3/2/24 1:12:00 PM

Page 13: [68] Deleted Cynthia Nevison 3/2/24 1:12:00 PM

Page 13: [68] Deleted Cynthia Nevison 3/2/24 1:12:00 PM

Page 13: [68] Deleted Cynthia Nevison 3/2/24 1:12:00 PM

Page 13: [69] Formatted Cynthia Nevison 3/11/24 10:39:00 AM

Font: 12 pt

Page 13: [69] Formatted Cynthia Nevison 3/11/24 10:39:00 AM

Font: 12 pt

Page 13: [69] Formatted Cynthia Nevison 3/11/24 10:39:00 AM

Font: 12 pt

Page 16: [70] Deleted Cynthia Nevison 3/3/24 10:49:00 AM

Page 16: [70] Deleted Cynthia Nevison 3/3/24 10:49:00 AM

Page 16: [70] Deleted Cynthia Nevison 3/3/24 10:49:00 AM

Page 16: [70] Deleted Cynthia Nevison 3/3/24 10:49:00 AM

Page 16: [70] Deleted Cynthia Nevison 3/3/24 10:49:00 AM

Page 16: [71] Deleted Cynthia Nevison 3/3/24 9:55:00 AM

Page 16: [72] Deleted Cynthia Nevison 3/3/24 2:28:00 PM

Page 16: [72] Deleted Cynthia Nevison 3/3/24 2:28:00 PM

Page 16: [72] Deleted Cynthia Nevison 3/3/24 2:28:00 PM

Page 16: [72] Deleted Cynthia Nevison 3/3/24 2:28:00 PM

Page 16: [73] Deleted Cynthia Nevison 3/3/24 2:34:00 PM

Page 16: [73] Deleted Cynthia Nevison 3/3/24 2:34:00 PM

▼
▲
Page 16: [73] Deleted Cynthia Nevison 3/3/24 2:34:00 PM

▼
▲
Page 16: [73] Deleted Cynthia Nevison 3/3/24 2:34:00 PM

▼
▲
Page 16: [73] Deleted Cynthia Nevison 3/3/24 2:34:00 PM

▼
▲
Page 16: [73] Deleted Cynthia Nevison 3/3/24 2:34:00 PM

▼
▲
Page 16: [73] Deleted Cynthia Nevison 3/3/24 2:34:00 PM

▼
▲
Page 16: [73] Deleted Cynthia Nevison 3/3/24 2:34:00 PM

▼
▲
Page 16: [73] Deleted Cynthia Nevison 3/3/24 2:34:00 PM

▼
▲
Page 16: [73] Deleted Cynthia Nevison 3/3/24 2:34:00 PM

▼
▲
Page 16: [73] Deleted Cynthia Nevison 3/3/24 2:34:00 PM

▼
▲
Page 17: [74] Deleted Cynthia Nevison 3/7/24 4:10:00 PM

▼
▲
Page 20: [75] Deleted Cynthia Nevison 3/5/24 3:39:00 PM

▼
▲
Page 20: [76] Deleted Cynthia Nevison 3/5/24 3:43:00 PM

▼
▲
Page 20: [77] Deleted Cynthia Nevison 3/4/24 3:24:00 PM

▼
▲
Page 26: [78] Deleted Cynthia Nevison 3/11/24 4:36:00 PM

▼
▲
Page 26: [79] Deleted Cynthia Nevison 3/11/24 4:37:00 PM

▼
▲
Page 27: [80] Deleted Cynthia Nevison 3/12/24 1:05:00 PM

▼
▲
x